6

Ultrashort Sources II: Examples

In the previous chapter the elements of passive mode-locking and their function for pulse shaping were described in detail. Analytical and numerical methods of characterizing mode-locked lasers were presented. Passive mode-locking is indeed the most widely applied and successful technique to produce pulses whose bandwidth approaches the limits imposed by the gain medium of dye and solid-state lasers including fiber lasers. Passive mode-locking was the technique of choice to produce sub 50-fs pulses in dye lasers and, today, is commonly applied in solid-state and fiber lasers. Sub 5-fs pulses have been obtained from Ti:sapphire lasers without external pulse compression [1] using this method.

In this chapter we will review additional techniques of mode-locking and discuss examples of mode-locked lasers. The purely active or synchronous mode-locking will be covered first, followed by the hybrid passive–active techniques. Other techniques not discussed in the previous chapter are additive mode-locking, methods based on second-order nonlinearities, and passive negative feedback. For their important role as saturable absorbers we will review the relevant properties of semiconductor materials. The last part of this chapter is devoted to specific examples of popular lasers.

6.1. SYNCHRONOUS MODE-LOCKING

A simple method to generate short pulses is to excite the gain medium at a repetition rate synchronized with the cavity mode spacing. This can be done by using a pump that emits pulses at the round-trip rate of the cavity or by pumped.

One of the main advantages of synchronous mode-locking is that a much broader

range of gain media can be used than in the case of passive mode-locking. This includes semiconductor lasers and, for instance, laser dyes such as oxazine 8, 9, and 14, which have too short a lifetime to be practical in cw operation, but are quite efficient when pumped with short pulses.

Ideally, the gain medium in a synchronously pumped laser should have a short lifetime, so that the duration of the inversion is not larger than that of the pump pulse. An extreme example is the case of optical parametric oscillators (OPO) where the gain lives only for the time of the pump pulse.

Synchronous pumping is sometimes used in situations that do not meet this criterion, just as starting mechanism. This is the case in some Ti:sapphire lasers, where the gain medium has a longer lifetime than the cavity round-trip time, and therefore synchronous pumping results in only a small modulation of the gain. The small modulation of the gain coefficient $a_0(t)$ is sufficient to start the pulse formation and compression mechanism by dispersion and SPM [2]. The initial small gain modulation grows because of gain saturation by the modulated intracavity radiation, resulting in a shortening of the function $a_0(t)$, and ultimately ultrashort pulses.

The simple considerations that follow, neglecting the influence of saturation, show the importance of cavity synchronism. If the laser cavity is slightly longer than required for exact synchronism with the pump radiation (train of pulses), stimulated radiation and amplified spontaneous radiation will constantly accumulate at the leading edge of the pulse, resulting in pulse distortions that could be even longer than the pump pulse. Therefore, to avoid this distortion, the cavity length should be slightly shorter than that required for exact synchronism with the pump radiation. Let us assume first perfect synchronism. The net gain factor per round-trip is

$$G(t) = e^{[a_0(t)d_0 - L]}, \tag{6.1}$$

where L is the natural logarithm of the loss per cavity round-trip. After a round-trips, the initial spontaneous emission of intensity I_{sp} has been amplified sufficiently to saturate the gain a_0, and thus the pulse intensity is approximately $I(t) \approx I_{sp} \propto \left[e^{(a_0(t)d_0 - L)}\right]^a$ or $I_{sp} \propto |G_0(t)|^a$. The pulse is thus $\sqrt{a}$ times narrower than the unsaturated gain function $G_0(t)$.

For a cavity shorter than required for exact synchronism, in a frame of reference synchronous with the pulsed gain $a_0(t)$, the intracavity intensity of the j^{th} round-trip is related to the previous one by:

$$I_j(t) = I_{j-1}(t + \delta)e^{[a_0(t)d_0 - L]}, \tag{6.2}$$

where δ is the mismatch between cavity round-trip time and the pump pulse spacing. The net gain for the circulating pulse $e^{[a_0(t)d_0 - L]}$ exists in the cavity for

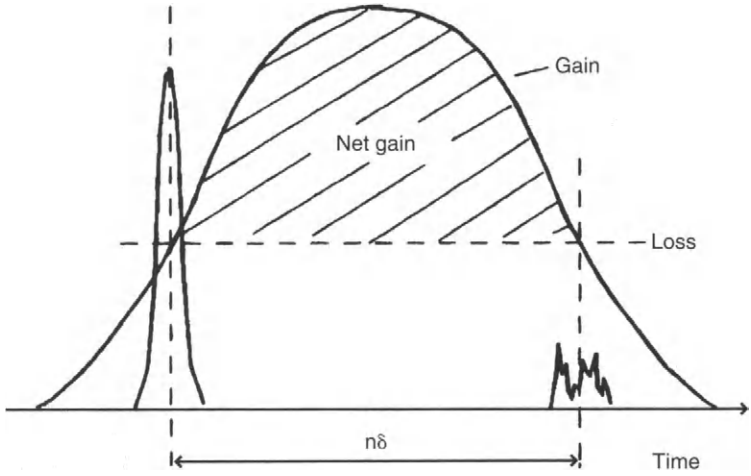

Figure 6.1 Net gain (gain minus loss) temporal profile as it appears at each periodicity of the pump pulse. If the round-trip time of the laser cavity is slightly shorter (by δ) than the pump period, emission appears at the right edge of the gain profile with respect to the last by the amount δ of each successive round-trip. A pulse will experience gain for a maximum of a period given by the width of the intensity of the gain divided by the difference δ.

a time $\pm\delta$ only, as can be seen from Figure 6.1. The laser oscillation will start from a small noise burst $I_{sp}(t)$. The intracavity pulse after n round trips can be approximated by:

$$I(t) = I_{sp}(t + n\delta)\left[e^{\langle \alpha_g \rangle_n - L}\right]^n, \tag{6.3}$$

where $I_{sp}(t + n\delta)$ is the spontaneous emission noise present in the cavity in the time interval $(n-1)\delta \to n\delta$, and $\alpha_m = \frac{1}{n\delta}\int \alpha_g(t)dt$ is a gain coefficient averaged over the n round-trips.

These simple considerations indicate that in the absence of any spectral filtering mechanism and neglecting the distortion of the gain curve $\alpha_g(t)$ by saturation, the pulse should be roughly $\sqrt{n}$ times shorter than the duration of the gain window. The timing mismatch δ is an essential parameter of the operation of a synchronously mode-locked laser. The shape of the autocorrelation (see Chapter 9) is typically a double-sided exponential, which—as pointed out by Van Stryland [3]—is a signature for a possible random distribution of pulse duration in the train. The interferometric autocorrelation also indicates a random (Gaussian) distribution of pulse frequencies [4]. These fluctuations in pulse duration and frequency have also been observed in theoretical simulations by Nisa and Cotterill [5] and Sauter [6].

Gain saturation—neglected in the elementary model discussed so far—does play an essential role in pulse shaping and compression for synchronously pumped lasers. We refer to a paper by Nakatsuka *et al.* [7] for a detailed review of the various theories of synchronous pumping. In a typical synchronously pumped laser, the net gain (at each round-trip) is "terminated" by gain depletion at each passage of the circulating pulse. The shortening of the gain period results in a laser pulse much shorter than the pump pulse. This mechanism was analysed in detail by Peiro *et al.* [8]. It has been verified experimentally that the shortest pulse duration is approximately $\tau_p \approx \sqrt{\tau_{pump} T_{2g}}$ [9]. This result illustrates the fact that the finite spectral width of the gain profile, $\Delta\nu_g \approx T_{2g}^{-1}$, ultimately limits the shortest obtained pulse duration. Numerical simulations have been made to relate the number of round-trips required to reach steady state to the single-pass gain [10].

Regenerative Feedback

As we have seen at the beginning of the previous section, the laser cavity should never be longer than the length corresponding to exact synchronism with the pump radiation to generate pulses shorter than the pump pulse. This implies strict stability criteria for the pump laser cavity, its mode-locking electronics, and the laser cavity (invar or quartz rods were generally used for synchronously pumped dye laser cavities). Considerations of thermal expansion of the support material and typical cavity lengths clearly show the need for thermal stability. Indeed, the thermal expansion coefficient of most rigid materials for the laser support exceeds 10^{-5}/°C. Because the cavity length approaches typically 2 m, even a temperature drift of 0.5°C would bring the laser out of its stability range. However, because it is the *relative* synchronism of the laser cavity with its pump source that is to be maintained, a simple and efficient technique is to use the noise (longitudinal mode beating) of the laser itself to drive the modulator of the pump laser [11] if the latter is actively mode-locked. This technique, sometimes called "regenerative feedback," has been applied to some commercial synchronously pumped mode-locked lasers, and even to a Ti:sapphire laser [2].

Seeding

Even if somewhat oversimplified, the representation of Fig. 6.1 gives a clue to an important source of noise in the synchronously pumped dye laser. The seed $I_{sp}(t)$ has a complex electric field amplitude $\tilde{s}(t)$ with random phase. As pointed out in Cathcart and Nave [12] and in Stamer [6] it is this spontaneous emission source that is at the origin of the noise of the laser. Could the noise be reduced by adding to $\tilde{s}$ a minimum fraction $\eta\tilde{E}(t)$ of the laser output, just large enough so that the phase of $\alpha\tilde{E}(t) + \tilde{s}(t)$ is equal to the phase of the output

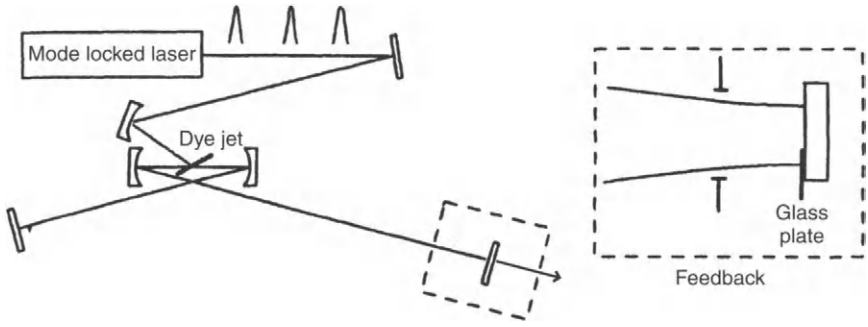

Figure 6.2 Typical synchronously pumped dye laser. The length of the dye laser cavity has to be matched to the repetition rate of the pump pulses. The noise in a synchronously pumped laser can be reduced by reinjection of a portion of the output chirped of the main intracavity pulse. A thin glass plate on the output chirped mirror(s) and reflects part of the beam into the cavity with the desired advance. The fraction of energy reflected (of the order of 10^{-3}) is determined by the coatings of the mirrors and the glass plate. (Adapted from Fesser *et al.*, [13].)

fields $\delta E(t)$ (which essentially implies $\eta E(t) \gg \bar{n}$)? Both calculation and experiment have demonstrated a dramatic noise reduction by sending the cavity with a small fraction of the pulse $\Delta\tau$ (leftover) of the main pulse. [13]. The emphasis here is on small; only a fraction of the order of 10^{-2} (and attenuating 10^{-3}) of the output power should be reinjected. A possible implementation would consist of collecting back a fraction of the output pulse delayed by slightly less than a cavity round-trip. This amounts to a weakly coupled external cavity. A much simpler implementation demonstrated by Fesser *et al.* [13] consists in inserting a thin glass plate (microscope cover glass for instance) in front of the output mirror (Figure 6.2). The amount of light reinjected is adjusted by translating the glass plate in front of the beam. The timing of the reinjected signal is determined by the thickness of the plate.

6.2. HYBRID MODE-LOCKING

Synchronous pumping alone can be considered as a good source of pulses rather than is perfect. The disadvantages of this technique, as compared to passive mode-locking, are:

- a longer pulse duration,
- larger amplitude and phase noise,
- the distribution of the pulses of the train are often evidently distributed, [3] and

- when attempting to achieve the shortest pulse durations, the pulse frequencies are randomly distributed [4].

One solution to these problems is to combine the techniques of passive and active mode-locking in a hybrid system [14,15]. Depending on the optical thickness of the absorber, the hybrid mode-locked laser is either a synchronously mode-locked laser perturbed by the addition of saturable absorption or a passively mode-locked laser pumped synchronously. The distinction is obvious to the user. The laser with little saturable absorption modulation will have the noise characteristics and cavity length sensitivity typical of synchronously pumped lasers, but a shorter pulse duration. The laser with a deep passive modulation (concentrated saturable absorber dye, or a large number of MQW for a semiconductor saturable absorber) shows intensity autocorrelation traces identical to those of the passively mode-locked laser [16]. The sensitivity of the laser to cavity detuning decreases. The reduction in noise can be explained as being related to the additional timing mechanism introduced by the absorber, which partially compensates the pulse advancing influence of the gain and spontaneous emission [17].

6.3. ADDITIVE PULSE MODE-LOCKING

6.3.1. Generalities

There was in the late 1980s a resurrection of interest in developing additive pulse mode-locking (APML), a technique involving coupled cavities. One of the basic ideas—to establish the weak coupling outside the main laser resonator—was suggested in 1965 by Foster *et al.* [18] and applied to mode-locking a He-Ne laser [19]. In that earlier implementation, an acousto-optic modulator is used to modulate the laser output at half the intermode spacing of the laser. The frequency shifted beam is reflected back through the modulator, resulting in a first-order diffracted beam, which is shifted in frequency by the total mode spacing, and reinjected into the laser cavity through the output mirror. The output mirror of the laser forms, with the mirror used to reinject the modulated radiation, a cavity with the same mode spacing as the main laser cavity. If the laser is close to threshold, a small intracavity modulation fed back into the main cavity can be sufficient to lock the longitudinal modes.

Unlike this technique more recent APML implementations are based on passive methods. In the purely dispersive version, pulses from the coupled cavity are given some phase modulation, such that the first half of the pulse fed back into the laser adds in phase with the intracavity pulse, while the second half

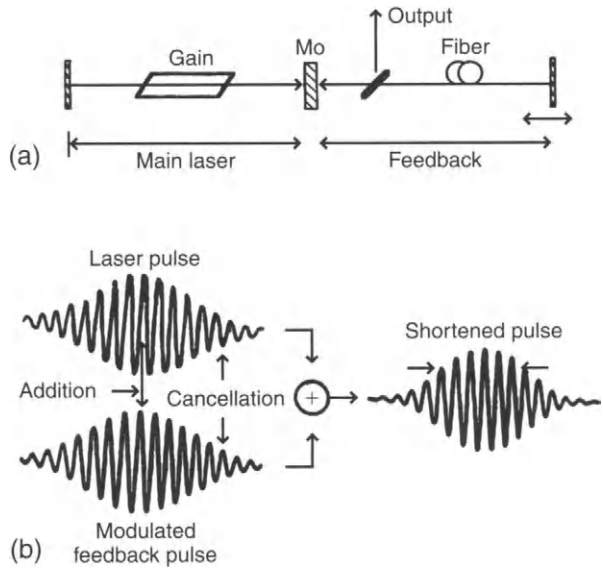

Figure 6.3 A typical additive pulse mode-locked laser cavity. At the output mirror Mo, the pulse of the main cavity [the fast leg] must coincide with the pulse of the auxiliary cavity [the slow leg] to create a shortened pulse [the right]. (Courtesy E. Wheeler.)

have opposite phase [20]. At each round-trip, the externally injected pulse thus contributes to compress the intracavity pulse, by adding a contribution on the leading edge and subtracting a certain amount from the trailing edge, as sketched in Figure 6.3. This technique has thus been applied to shortening pulses generated through other mode-locking mechanisms. A reduction in pulse duration by as much as two orders of magnitude was demonstrated with color-center lasers [21–24] and with Ti:sapphire lasers [25].

It was subsequently realized that the mechanism of pulse addition through a nonlinear coupled cavity is sufficient to passively mode-lock a laser. This technique has been successfully demonstrated in a Ti:sapphire laser [26] Nd:YAG [27,28] Nd:YLF [29,30], Nd:glass [31], and KCl color-center lasers [32]. A detailed description of the coherent addition of pulses from the main laser and the extended cavity which takes place in the additive pulse mode-locking has been summarized by Ippen *et al.* [33].

Coherent field addition is only one aspect of the coupled cavity mode-locked laser. The nonlinearity from the coupled cavity can be, for example, an amplitude modulation, as in the "soliton" laser [34], or a saturable nonlinear reflectivity via a quantum well reservoir [35].

6.3.2. Analysis of APML

Analysis of APML [23,33] has shown that the coupling between a laser and an external auxiliary cavity can be modeled as an intensity-dependent reflectivity of the laser end mirror. Let r be the real (field amplitude) reflection coefficient of the output mirror. The radiation transmitted through that mirror into the auxiliary (external) cavity returns to the main cavity having experienced a field amplitude loss γ ($\gamma < 1$) and a total phase shift $-[\phi + \Phi(t)]$. The nonlinear phase shift $\Phi(t)$ induced by the nonlinearity is conventionally chosen to be zero at the pulse peak [33] so that the linear phase shift ϕ includes a bias because of the peak nonlinear phase shift. Therefore, if $r\tilde{E}(t)$ is the field reflected at the mirror, the field transmitted through the output mirror, the auxiliary cavity (loss γ) and transmitted a second time through the output mirror is $(1-r^2)\gamma e^{-i\Phi}\tilde{E}(t)e^{-i\Phi(t)}$. If ϕ is the length of the nonlinear medium, and assuming a Kerr nonlinearity, according to Eq. (3.149):

$$\Phi(t) = \frac{2\pi}{\lambda_0}\bar{n}_2 z\,[I_{aux}(t) - I_{aux}(0)]\phi \tag{6.4}$$

where $I_{aux}(t)$ is the intensity of the field in the auxiliary cavity. For a qualitative discussion we determine the total reflection by adding the contribution of the reinjected field from the auxiliary cavity to the field reflection r of the output mirror, which leads to a time-dependent complex "reflection coefficient" $\tilde{\Gamma}$:

$$\tilde{\Gamma}(t) \approx r + \gamma(1-r^2)e^{-i\phi}[1 - i\Phi(t)]. \tag{6.5}$$

In Eq. (6.5), it has been assumed that Φ is small, allowing us to substitute for the phase factor $e^{-i\Phi}$ its first-order expansion. There is a differential reflectivity for different parts of the pulse. If one sets $\phi = -\pi/2$, then $|\tilde{\Gamma}|$ has a maximum value at the pulse center where $\Phi = 0$, and smaller values in the wings:

$$\tilde{\Gamma}(t) \approx r + \gamma(1-r^2)\Phi(t) + i[\gamma(1-r^2)]. \tag{6.6}$$

The reflection is thus decreasing when Φ becomes negative in the wings of the pulse, which is the "chirped field interaction" sketched in Fig. 6.3. The compression factor is determined by the ratio of $\gamma(1-r^2)$ to r, which can be related to the ratio of energy in the auxiliary cavity to that in the main cavity [note that $\gamma(1-r^2)$ is the normalized amount of energy that can be subtracted from the pulse in the main cavity at each round-trip].

This dynamic reflectivity can be adjusted for pulse shortening at each reflection, until a steady-state balance is achieved between the pulse shortening and pulse lengthening because of bandwidth limitation and dispersion.

6.4. MODE-LOCKING BASED ON NONRESONANT NONLINEARITY

Various techniques of mode-locking using second-order nonlinearities have been developed. A first method is a direct extension of Kerr lens mode-locking, which has been analyzed in the previous chapter. A phase third-order susceptibility can be found near phase matching conditions in SHG, not unlike the situation encountered with a third-order susceptibility, which is said to be enhanced near a two photon resonance [36,37]. In this method, called extended second-order nonlinearity mode-locking, the nonlinear crystal is used in mismatched conditions with a mirror that reflects totally both the fundamental and SH waves. The cascade of sum and difference frequency generation induces a transverse focusing of the fundamental beam in a way similar to Kerr self-focusing. This method has been applied to solid-state lasers by Cerullo *et al.* [38] and Dascalov *et al.* [39]. The resonance condition (the phase matching bandwidth) implied in this method does not make it applicable to the fs range.

Another technique was introduced by Sarukov, [40,41] who demonstrated passive mode-locking in a Q-switched laser by means of a nonlinear mirror consisting of a second harmonic generating crystal and a dichroic mirror. Dispersion between the crystal and the dichroic mirror is adjusted so that the reflected SH is converted back to the fundamental.

A third method, based on polarization rotation occurring with type II second harmonic generation, is the equivalent of Kerr lens mode locking in fiber lasers. It has also been applied to some solid-state lasers. The last two methods will be discussed in more detail in the following subsections.

6.4.1. Nonlinear Mirror

The principle of operation of the nonlinear mirror can be understood with the sketch of Figure 6.4, showing the end cavity elements that provide the function of nonlinear reflection. A frequency doubling crystal in phase matched orientation

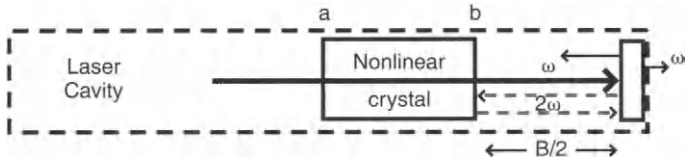

Figure 6.4 End cavity assembly containing a nonlinear mirror. The end mirror is a total reflector for the SH and a partial reflector for the fundamental.

is combined with a dichroic mirror output coupler that totally reflects the SH beam and only partially reflects the fundamental. These two elements form a reflector, whose reflectivity at the fundamental wavelength can either increase or decrease, depending on the phases of the fundamental and SH radiation. These phase relations between the first and second harmonics can be adjusted inserting a dispersive element between the nonlinear crystal and the dichroic mirror. The dispersive element can be either air (the phase adjustable parameter is the distance between the end mirror and the crystal) or a phase plate (of which the angle can be adjusted).

At low intensity, the cavity loss is roughly equal to the transmission coefficient of the output coupler at the fundamental wavelength. At high intensities, more second harmonic is generated, reflected back and reconverted to the intracavity fundamental, resulting in an increase in the effective reflectance coefficient of the crystal-output coupler combination. The losses are thus decreasing with intensity, just as is the case with a saturable absorber. Figure 6.5 shows the variation of intensities of the fundamental and second harmonic in the first (left) and second (right) passage through the second harmonic generating crystal. Depletion of the

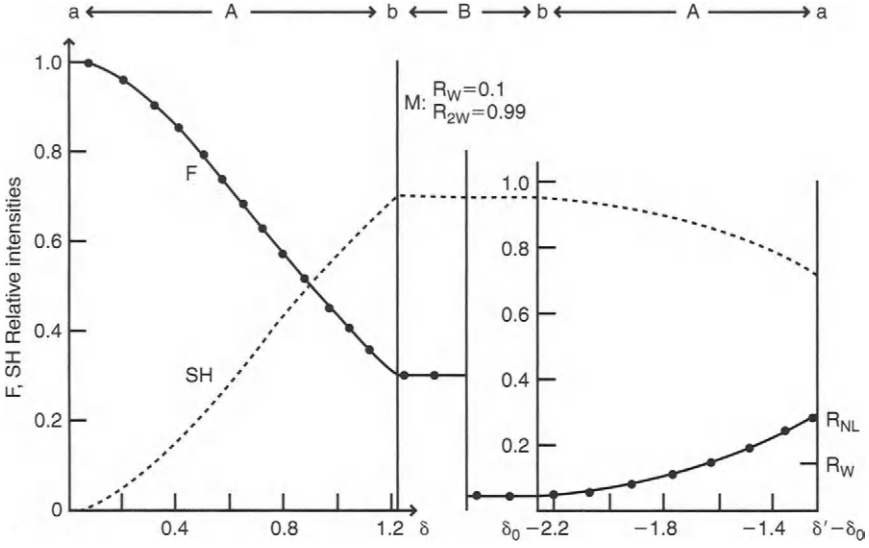

Figure 6.5 Variation of intensity of the fundamental (F, solid line) and the second harmonic (SH, dashed line) in two successive passages. A and B designate the nonlinear crystal. The solid and dashed curves are identical to Fig. 6.4. A fraction $R_W = 10\%$ of the fundamental radiation is reflected back into the crystal, together with the native second harmonic. After propagation for a distance δ in air, the phase δ' of the second harmonic with respect to the fundamental has undergone a shift of π, resulting in a reconversion of second harmonic into fundamental on the second passage.

fundamental through SHG reduced the intensity to 30% of its initial value. Only 10% of that fundamental is reflected back through the second harmonic generating crystal. However, because the full SH signal that was generated in the first passage is reflected back, and because it has returned phase with respect to the fundamental, 30% of the initial fundamental is recovered. At the first passage, the conversion to second harmonic should be sufficient to have a sizeable depletion of the fundamental. Therefore, this method works best for high-power lasers. The theoretical framework for the SHG has been set in Chapter 3 (Section 3.4.1) and can be applied for a theoretical analysis of this type of mode-locking. A frequency domain analysis of the mode-locking process using a nonlinear mirror can be found in Stankov [42]. Available software packages, such as—for example—*SNLO* software can be used to compute the conversion of fundamental and second harmonic at each passage [43].

The electronic nonlinearity for harmonic generation responds in less than a few femtoseconds. However, because of the need to use long crystals to obtain sufficient conversion, the shortest pulse durations that can be obtained by this method are limited to the picosecond range by the phase matching bandwidth. The method has been applied successfully to flashlamp pumped lasers [44] and diode pumped lasers [45–48]. A review can be found in Kubecek [49].

The same principle has also been applied in a technique of parametric mode-locking, which can be viewed as a laser hybridly mode-locked by a nonlinear process [50]. The third-order nonlinearity of a crystal applied to sum and difference frequency generation is used in the mode-locking process. The nonlinear mirror can also be used to provide negative feedback instead of positive feedback by adjusting the phase shift between fundamental and second harmonic by the dispersive element [51].

6.4.2. Polarization Rotation

Nonlinear polarization rotation because of the nonlinear index associated with elliptical polarization has been described in Section 3.4.2 as an example of a third-order nonlinear process. Again, a second-order nonlinearity can also be used for polarization rotation. As is the case when phase matched SHG is used, the minimum pulse duration is determined by the inverse of the phase matching bandwidth.

Under type II phase matching, the orientation of the fundamental field polarization (assumed to be linear) at the output of the nonlinear crystal is directly dependent on the relative intensity of the two orthogonal polarization components. The crystal cut and orientation is assumed to perfectly fulfill the phase matching conditions for SHG if the linearly polarized incoming field is split into two orthogonal components with exactly equal intensity, then the wave of

smallest initial amplitude may be completely depleted because the SHG process diminishes each component by the same amount. If the nonlinear propagation continues beyond that point the SHG is replaced by difference frequency generation between the generated harmonic and the remaining fundamental component. The new fundamental field appears on the polarization axis where the fundamental had disappeared but the phase of the created field is now shifted by π with respect to the initial field. Difference frequency generation then goes on with propagation distance until the power of the second harmonic goes to zero. If we assume that the crystal behaves in the linear regime like a full-wave or half-wave plate then the output polarization state remains linear in the nonlinear regime, but the attenuation of the output is intensity dependent. Two properly oriented polarizers placed on either side of the nonlinear crystal permit us to build a device with an intensity dependent transmission.

Details on the use of nonlinear polarization in a type II SHG for mode-locking of a cw lamp pumped Nd:YAG laser are given in Kubecek *et al.* [52].

6.5. NEGATIVE FEEDBACK

In this section we will describe a technique that limits the peak power of pulses circulating in the cavity. This can be accomplished by a combination of an element producing nonlinear defocusing and an aperture. Negative feedback has gained importance in Q-switched and mode-locked solid-state lasers because it tends to lengthen the pulse train by limiting the peak power and thereby reducing the gain depletion. Moreover, a longer time for pulse formation usually leads to shorter output pulses and more stable operation.[1]

We have seen that the pulse formation—in positively mode-locked lasers—is associated with a positive feedback element (Kerr lensing, saturable absorber) which enhances positive intensity fluctuations (generally through a decrease of losses with increasing intensity). Although a positive feedback leads to pulse formation, it is inherently an unstable process, because intensity fluctuations are amplified. Therefore, it is desirable, in particular in high-power lasers, to have a negative feedback element that acts at higher intensities than the positive feedback element.

Pulses of 16, 3, and best than 1 ps have been generated with this technique with Nd:YAG, Nd:YAP, and Nd:glass lasers, respectively. Most importantly for the fs field, the pulse-to-pulse reproducibility (better than 0.2% [53]) makes these lasers ideal pump sources for synchronous or hybrid mode-locking. The flashlamp pumped solid-state laser with negative feedback provides a much higher energy

[1] Note that in high-power solid-state lasers the typical Q-switched pulse is not much longer than a few cavity roundtrips.

per pulse, at shorter pulse duration, than the cw mode-locked laser used conventionally as pump for fs systems. The use of negative feedback to efficiently pump a fs dye laser was demonstrated by Knight et al. [10].

In semiconductor laser pumped solid-state lasers, negative feedback can be used to suppress Q-switched mode-locked operation, in favor of cw mode-locked operation [54]. The mechanism is the same as for the flashlamp pumped laser: the energy limiting prevents the total gain depletion that ultimately interrupts the pulse train.

Electronic Feedback

A typical flashlamp pumped, mode-locked Nd laser generates a train of only 5 to 10 pulses of all different intensities. In the first implementation of "negative feedback," an electronic feedback loop monitored the cavity losses, if the pulse energy exceeds a well-defined value. Martinez and Spinelli [55] proposed to use an electro-optic modulator to actively limit the intracavity energy in a passively mode-locked glass laser. They demonstrated that the pulse train could be extended. A fast high voltage electronics led to the generation of μs pulse trains in a passively mode-locked glass lasers [56] and in hybrid Nd:glass lasers [57].

Electronic Q-switching and negative feedback has the advantage that the clamping of the pulses is electronically controlled. This is important in applications where several laser systems have to be synchronized. However, there is a minimum response time of one cavity round-trip before the feedback can react [57].

Passive Negative Feedback

A passive feedback system can provide instantaneous response—i.e., on the time scale of the pulse rather than on the time scale of the cavity round-trip. We will here restrict our description to the Nd laser using a semiconductor (GaAs) for passive negative feedback. The semiconductor used in a passive feedback system produces nonlinear lensing. The analysis of the beam focusing is identical to that of the Kerr lensing, except that the sign of the lensing is opposite. The nonlinear index change is initiated by electrons generated by two photon absorption into the conduction band. Various processes then contribute to the index change. The index change by free electrons, for example, can be estimated with the Drude model and is negative:

$$\Delta n_{eh}(t, r, l) = -\frac{Ne^2}{2m^* \varepsilon_0 \omega_l^2} N(x, y, t), \tag{6.7}$$

where N is the electron density, m^* is the electron's effective mass and ε_0 is the linear index. We refer to the literature for additional contributions to Δn such as the interband contribution [58] and an additional electronic contribution [36,59].

Other implementations of passive negative feedback have used a SH crystal near phase matching ("cascaded nonlinearity") to produce a large nonlinear index required for the energy limiter [60].

A typical laser using passive negative feedback generally includes a saturable absorber for Q-switching and mode-locking and an energy limiter. An energy limiter that can be used for passive negative feedback is illustrated in Figure 6.6. A two photon absorber (typically GaAs) is located near a cavity end mirror. After double passage through this sample, the beam is defocused by a self-induced lens originating mainly from the free carriers generated through two photon absorption. The defocused portion of the beam is truncated by an aperture. Self-defocusing in the semiconducting two photon absorber sets in at a power level that should be close to the saturation intensity of the saturable absorber used for Q-switching and mode-locking. Because the pulse intensity is close to the pulse saturation intensity, there is optimal pulse compression at the pulse leading edge by saturable absorption. Because of self-defocusing in GaAs, the pulse trailing edge is clipped off, resulting in further pulse compression and energy loss.

The stabilization and compression of the self-mode pulses result from a delicate balance of nonlinear physical mechanisms. Details of the experimental implementation and theoretical analysis can be found in the literature [41–63].

At the end of this section we will discuss an experiment that illustrates the saturable and limiting properties of a particular nonlinear element. Often the nonlinear element is just the substrate of a multiple quantum well [54]. In that case, one has correlated the function of saturable absorber (the MQW, excited by one photon absorption) and energy limiter (the substrate, excited by two photon absorption). The properties of the MQW as the substrate and well demonstrated by the measurement illustrated in Figure 6.7 and 6.8. A diode pumped microchip YAG laser is used to focus pulses of 3 μJ energy and 1 ns duration at a repetition rate of 15.26 kHz into a sample consisting of 100 quantum

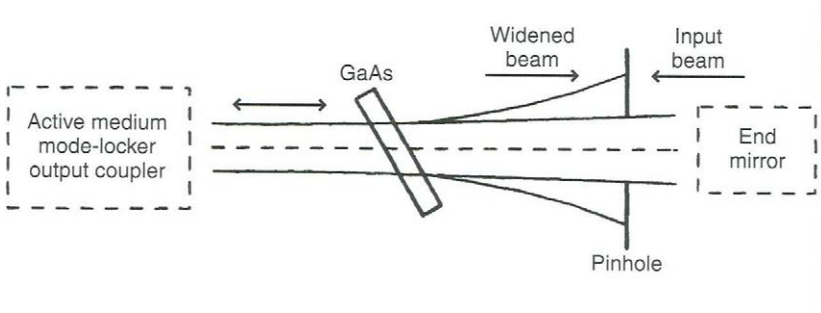

Figure 6.6 Passive negative feedback is typically achieved by inserting in the cavity an energy limiter, which can consist of a GaAs plate working as two photon absorber with subsequent defocusing element, and an aperture (pinhole).

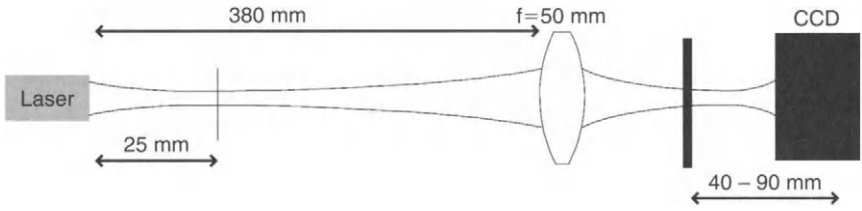

Figure 6.7 Experimental setup to observe the saturable absorption, two photon absorption and self-lensing in a sample of 100 quantum wells on a GaAs substrate located in front of a CCD camera (from Kubecek *et al.* [64]).

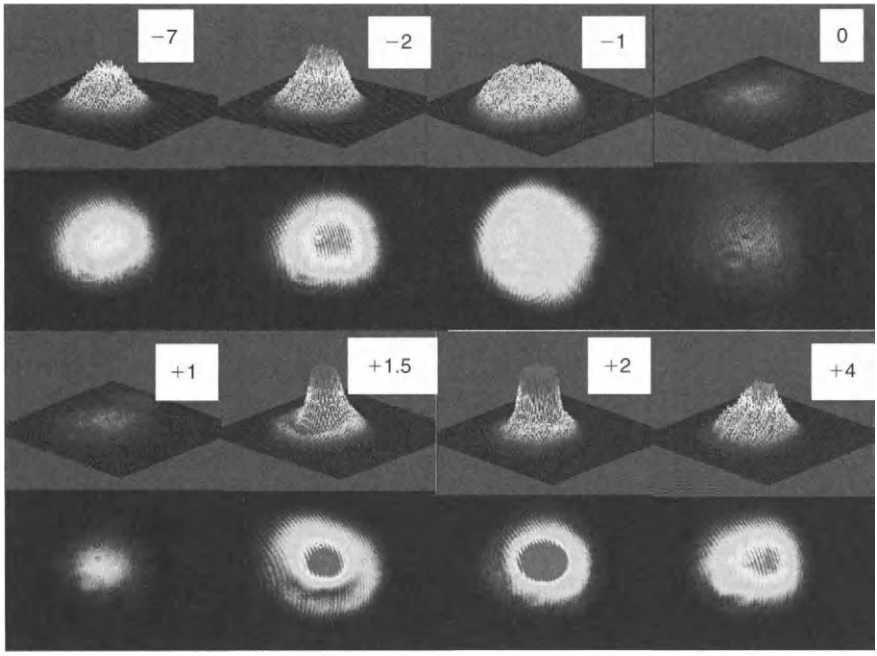

Figure 6.8 Spatial beam structure versus longitudinal position of the sample along the axis of the beam, after the lens. The distances from focus are indicated (in mm). The upper part of the figure corresponds to the positions left of the focus; the lower part right of the focus. (Adapted from Kubecek *et al.* [64].)

wells on a GaAs substrate. The lens has a focal distance of 50 mm. The output power from the laser was attenuated not to damage the MQW. The maximum power density in the focal point was 10 MW/cm^2. The spatial profile of the radiation transmitted through the sample was analyzed, using a CCD camera, as a function of the position of the sample. The various profiles are shown in Fig. 6.8. From this picture we can see that the initial low power transmission of 23% far from the focal point increases to 43% close to the focal point. The transmission of the GaAs plate alone is 53%, indicating that the unsaturable losses in the MQW are about 10%. The increase in transmission reflects the saturation of the quantum wells. Close to the focal point, the transmission drops and significant defocusing is observed. This is a region of large two photon absorption, creating an electron plasma sufficiently dense to scatter the beam. Self-defocusing is observed with the sample positioned to the left of the focus, self-focusing to the right of the focus.

6.6. SEMICONDUCTOR-BASED SATURABLE ABSORBERS

Progress in the fabrication of semiconductors and semiconductor based heterostructures, such as MQWs, has led to the development of compact and efficient saturable absorbers whose linear and nonlinear optical properties can be customized. These devices are particularly suited for mode-locking solid-state lasers, fiber lasers and semiconductor lasers. They can conveniently be designed as fast absorbers, which makes them attractive for initiating and sustaining mode-locking in a variety of subpicosecond lasers and cavity configurations. For a review see Keller *et al.* [65].

In semiconductors a transition from the valence to the conduction band is mostly used. In MQWs an excitonic resonance near the band edge can be utilized [66], which leads to a lower saturation energy density [67].

As discussed in the previous chapter an important parameter is the relaxation time of the absorber. The recovery rate is the sum of the carrier relaxation rate $1/T_1$ and the rate of diffusion out of the excited volume $1/\tau_d$:

$$\frac{1}{\tau_A} = \frac{1}{T_1} + \frac{1}{\tau_d}. \tag{6.38}$$

For a beam waist w_0 in the absorber the characteristic diffusion time can be calculated by

$$\tau_d = \frac{w_0^2}{8D}.$$

where D is the diffusion constant, which is related to the carrier mobility μ through the Einstein relation $D = k_B T \mu / e$. For a beam waist of 2 μm and $D = 10$ cm^2/s for example, the diffusion time $\tau_d \approx 500$ ps.

Typical carrier lifetimes in pure semiconductors are ns and thus too long for most mode-locking applications, where the cavity round-trip time is of the order of a few ps. Several methods are available to reduce the effective absorption recovery rate of bulk semiconductors and MQWs:

1. rapid trapping and
2. injection of defects.

A commonly used technique to insert defects is proton bombardment with subsequent proton annealing. For example, the bombardment of a MQW sample consisting of 80 pairs of 100 Å GaAs and 101 Å $GaAs_{0.71}Al_{0.29}As$ wells, with 200-keV protons resulted in recovery times of 360 ps and 150 ps, respectively [67]. Structures with thinner wells (70 to 80 Å) separated by 100 Å barriers yield broader absorption bands [68], with the same recovery time of 150 ps after a 10^{13}/cm^2 proton bombardment and annealing.

Another technique to introduce defects is to grow the semiconductor at relatively low temperatures. This can lead to a relatively large density of deep-level defects that can quickly trap excited carriers. As an example, Figure 6.9 shows

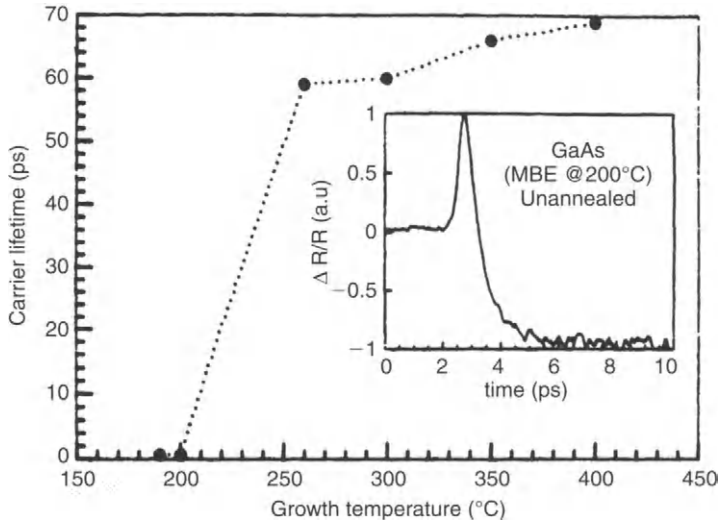

Figure 6.9 Carrier lifetime of GaAs versus MBE growth temperature. The inset shows the transient reflection measured in a pump-probe experiment for a 200°C grown unannealed sample. (Adapted from Chyon *et al.* [69])

Table 6.1

Semiconducting materials with carrier lifetimes and mobilities. (Adapted from Gupta *et al.* [69].)

Material	Carrier lifetime T_1 (ps)	Mobility μ (cm^2/Vs)
Cr-doped GaAs	50–100	1000
Ion implanted InP	3–4	200
low-damaged Si-on-sapphire	0.6	30
Amorphous silicon	0.3–30	1
MOCVD CdTe	0.45	280
GaAs (MBE, 200°C)	0.3	120
$In_{0.53}Al_{0.48}As$ (MBE, 150°C)	0.4	5

a plot of the carrier lifetime versus MBE growth temperature. The measurement is performed by focusing a 100 fs pump pulse onto a 20–30 μm spot on the semiconductor. A 10 times attenuated (as compared to the pump) probe pulse is focused into a 10 μm island within the pumped region. Both pump and probe are at 620 nm. The reflectance of the probe is measured as a function of probe delay (inset in Fig. 6.9). The carrier lifetime is defined as the initial decay (1/e) of the reflectance versus delay.

Table 6.1 lists carrier lifetimes and mobilities of some representative semiconductor materials.

6.7. SOLID-STATE LASERS

6.7.1. Generalities

Most common solid-state lasers used for ultrashort pulse generation use materials with a long lifetime (compared to typical cavity round-trip times) as gain media. The laser efficiency can be high if pumped by other lasers, for example semiconductor lasers, tuned to the pump transition. This is especially the case for lasers such as Ytterbium YAG that have a small quantum defect.[2]

Because these solid-state lasers have small gain cross sections as compared to dye lasers and semiconductor lasers, gain modulation is ineffective

[2]The quantum defect is the difference in energy of the pump photon and the laser emitting photon.

for mode-locking. With an upper state lifetime many orders of magnitude longer than the round-trip time, synchronous pumping is seldom used.[3]

The relatively low gain cells for longer lasing media, of the order of several mm, as opposed to the typical 100 μm used with dye and semiconductor lasers. The long gain crystal in such systems helps SPM. Therefore, mode-locking will most often occur through Kerr lensing and chirping in the gain medium. Some examples where saturable absorbers are used are:

- Long pulse generation, tunable in wavelength.
- Mode-locking of LiCAF lasers, where the Kerr effect is small.
- Bidirectional mode-locking of ring lasers. (Kerr lensing in the gain medium favors unidirectionality).

Also because of the longer gain medium, as compared to dye and semiconductor lasers), the laser will be sensitive to any parameter that influences the index of refraction. These are:

- Laser pulse intensity—an effect generally used for passive mode-locking (Kerr lensing).
- Temperature dependence of the index of refraction, which leads to thermal lensing and birefringence.
- Change in index of refraction associated with the change in polarizability of optically pumped active ions.

The latter effect was investigated by Powell *et al.* [70] in Nd-doped lasers, and found to be of the order of 30% of the thermal change in index.

Pumping of solid-state lasers is done either by another laser (for instance argon ion laser, or frequency doubled vanadate (YVO_4) laser, for Ti:sapphire) or by a semiconductor laser (Cr:LiSAF, Nd-vanadate) or by flashlamps (Nd:YAG). Diode laser pumping is the most advantageous from the point-of-view of wall plug efficiency.

Mode-locked solid-state lasers used as specialize according to the property that is desired. So far Ti:sapphire lasers have been the choice for shortest pulse generation and stabilized frequency combs. Diode pumped Cr:LiSAF lasers can reach pulse durations in the vicinity of fs and are the preferred laser when extremely low power consumption is desired. Nd:YAG lasers are most convenient for generating high-power Q-switched mode-locked ps pulse trains and are generally flashlamp pumped. Nd:vanadate is generally used as diode pumped Q-switched mode-locked source, although it is possible to achieve cw mode locked operation too. Both Nd:YAG and vanadate have a bandwidth that renders their operation

[3] Synchronous pumping was first used with Ti:sapphire lasers to provide the modulation necessary to start the Kerr lensing mode-locking, but, not as a primary mode-locking mechanism.

to a shortest pulse of approximately 10 ps. The laser with the lowest quantum defect is sought for high power application where efficiency is an issue. Yb:YAG can be pumped with 940 nm diode lasers as well as 1.05 microns. An optical to optical conversion efficiency of 35% has been obtained [71].

6.7.2. Ti:sapphire Laser

The Ti:sapphire laser is the most popular source of fs pulses. The properties that make it one of the most attractive source of ultrashort pulses are listed in Table 6.2. Ti:sapphire is one of the materials with the largest gain bandwidth, excellent thermal and optical properties, and a reasonably large nonlinear index.

Table 6.2

Room temperature physical properties of Ti:sapphire. The gain cross-section increases with decreasing temperature, making it desirable to operate the laser at low temperatures. The values for the nonlinear index from Sheikbahae and Wise [72] take into account the conversion factor of Eq. (3.149). Some data are given for σ (perpendicular to the optical axis) and π (parallel to the optical axis) polarizations.

Property	Value	Units	Reference
Index of refraction at 800 nm	1.76		[72]
Nonlinear index (Kerr coef.)	$\approx 3.5 \cdot 10^{-16}$	cm^2/W	[73]
Raman shift	419	cm^{-1}	[73]
Decay time T_R	8	ps	[73]
Raman contribution to β_2	$1.7 \cdot 10^{-17}$	cm^2/W	[73]
Raman shift	647	cm^{-1}	[73]
Decay time T_R	6	ps	[73]
Raman contribution to β_2	$0.8 \cdot 10^{-17}$	cm^2/W	[73]
Saturation (π) at 800 nm	612	J/cm^2	
Peak absorption at	500	nm	
σ_{abs}	$5.5 \cdot 10^{-20}$	cm^2	[74]
σ_{em}	$2.5 \cdot 10^{-20}$	cm^2	[74]
Number density of Ti^{3+} at a concentration of	$3.5 \cdot 10^{19}$ 0.1	cm^{-3} wt% Ti_2O_3	
Peak gain at	795	nm	
σ_{em}	$3 \cdot 10^{-19}$	cm^2	[74]
σ_{abs}	$1.7 \cdot 10^{-20}$	cm^2	[74]
Fluorescence lifetime τ_f	3.15	μs	[74]
dn/dT	-0.0065	$\mu s/K$	[74]

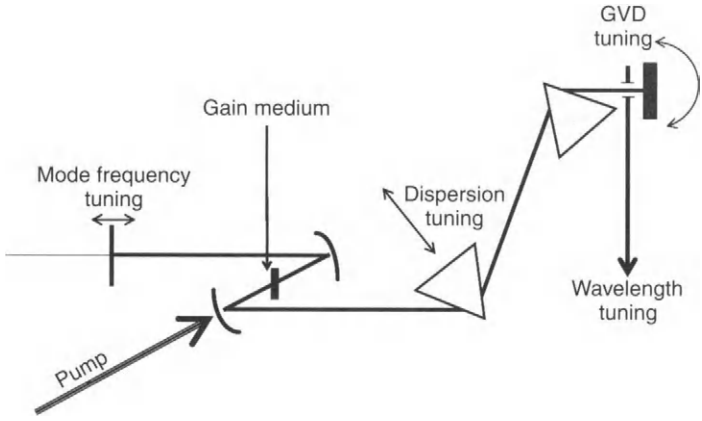

Figure 6.18 Typical Ti:sapphire laser cavity consisting (from the right) of an end mirror, an optional prism pair, folding mirrors at both sides of the laser crystal, and an output coupler. Flat mirrors evolve that are provided so that laser can be achieved.

A typical configuration is sketched in Figure 6.18. The pump laser is typically either a cw Ar ion laser or a frequency doubled Nd:vanadate laser. The operation of the Ti:sapphire laser is referred to as "self-mode-locked" [75]. The cavity configuration is usually linear, consisting only the active element (the Ti:sapphire rod), mirrors and dispersive elements. The latter can be a pair of prisms (cf. Section 2.5.5), or negative dispersion mirrors (cf. Section 2.3.3), or other laser-interferometric structures. Dispersion control by prisms [76] and by mirrors [77] led to the generation of pulses shorter than 12 fs in the early 90s. The output power typically can reach hundreds of mW at pump powers of less than 5 W. Sometimes, to start the pulse evolution and maintain a stable pulse regime, a saturable absorber, an acousto-optic modulator, a wobbling end mirror, or synchronous pumping is used.

The mode-locking mechanism most often exert in the cavity of Fig. 6.18 is Kerr lens mode-locking. The cavity mode is adjusted in such a way that the lasing effect in the Ti:sapphire rod results in a better overlap with the pump beam, hence an increased gain for high peak power pulses (soft aperture). Another approach discussed in Section 5.4.3 and Appendix E is to insert an aperture in the cavity. In a beneficial way the self-focusing results in reduced losses (increased transmission) through the aperture (hard aperture).

While Kerr lensing (a combination with a soft or a hard aperture) initiates the amplitude modulation essential to start the mode-locking, the succession of SPM and quadratic dispersion is responsible for pulse compression. The prism pair provides a convenient means to tune the dispersion to an optimal value that will

compensate the SPM, by translating the prism into the path of the beam, as shown in Fig. 6.10.

The shortest pulse duration that can be achieved is ultimately determined by higher-order dispersion, which includes a contribution from the prism material, from the Ti:sapphire crystal, and the mirror coatings. To minimize the third-order dispersion from the gain medium, short crystal lengths (2 to 4 mm) with the maximum doping compatible with an acceptable optical quality of the Ti:sapphire crystal are generally used. If the shortest pulses are desired, quartz prisms are generally preferred because of their low third-order dispersion. Moreover, because the second-order dispersion of quartz is also small, the shortest pulse is compromised against a long round-trip time, because the intracavity distance has to be large (>1 m) to achieve negative dispersion. Another choice of prism material is LaK16, which has a sufficient second-order dispersion to provide negative dispersion for distances of the order of 40 cm to 60 cm. Highly dispersive prisms such as SF10 or SF14 are used when a large number of dispersive intracavity elements has to be compensated with a large negative dispersion.

Several "control knobs" are indicated on the Ti:sapphire laser sketched in Fig. 6.10. After traversing the two prism sequence from left to right, the various wavelengths that constitute the pulse are displaced transversally before hitting the end mirror. An adjustable aperture located between the last prism and the end mirror can therefore be used either to narrow the pulse spectrum (hence elongate the pulse) or tune the central pulse wavelength. A small tilt of the end mirror—which can be performed with piezoelectric elements)—can be used to tune the group velocity (hence the cavity round-trip time, or the mode spacing) without affecting the optical cavity length or the average pulse frequency (no translation of the modes). The position of the modes—in particular the mode of the average pulse frequency—can be controlled by translation of the end mirror with piezoelectric transducers. Both a motion also affects the repetition rate of the cavity. Ideally, orthogonal control of the repetition rate and mode position requires two linear combinations of the piezo controls just mentioned.

Cavities with Chirped Mirrors

Instead of intracavity prisms, negative dispersion mirrors are the preferred solution for the shortest pulses, provided a short Ti:sapphire rod is available, and there is no other dispersive, intracavity element. Continuous tuning of the dispersion is not possible as was the case with the intracavity prism pair. Discrete tuning however is possible, through the insertion of multiple reflections on the dispersive mirrors. The minimum increment of dispersion is the dispersion associated with a single reflection.

As we saw in Chapter 5, one of the applications of mode-locked lasers is to generate frequency combs for metrology. We will discuss such examples, and the

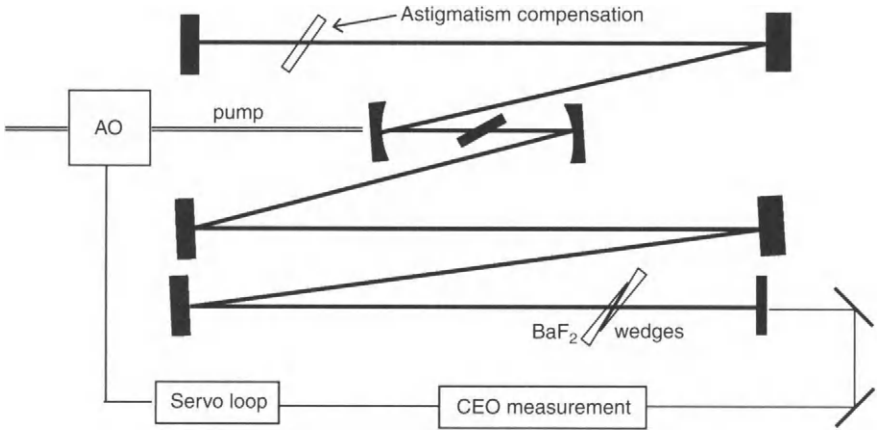

Figure 6.31 Ti:sapphire laser cavity with chirped mirrors for 5-fs pulse generation. Two wedges of BaF_2 are used for continuous dispersion control. The intracavity group velocity is tuned through the group linearity. The servo loop drives the signal from the measurement of the CEO, and feeds it back to the acousto-optic modulator. Adapted from Ell et al. [1].

lasers applied in more detail in Chapter 13. For these applications it is desirable to have an octave spanning pulse spectrum, which implies pulses as short as 3 fs or about two optical cycles [1]. This allows one to mix the second harmonic of the IR part of the mode comb with a mode from the short wavelength part of the fundamental spectrum—a technique to determine the carrier to envelope offset [78–81]. An example of such a 5-fs laser is sketched in Figure 6.31. Mirrors with a smooth negative dispersion over the whole spectrum have been developed (see Section 2.3.3) and double-chirped mirrors have been used for this laser [82]. Both the low and high index layers of these coatings are chirped. The spectral analysis of the reflectivity of these coatings will always "phase ripples." To eliminate these ripples, the mirrors are used in pairs, manufactured in such a way that the ripples are 180 degrees out of phase.

Continuous dispersion tuning is achieved by the use of thin BaF_2 wedges. BaF_2 is the material with a low ratio of third- to second-order dispersion in the wavelength range from 600 to 1200 nm, and the slope of its dispersion is nearly identical to that of air. It is therefore possible to scale the cavity to, for instance, shorter dimensions, and maintain the same dispersion characteristics by adding the appropriate amount of BaF_2.

High Power from Oscillators

For some applications, for example laser micromachining, it is desirable to increase the pulse energy of the output of fs oscillators without amplification.

Because the pump power is limited an increase in pulse energy can only be at the expense of repetition rate. Several different techniques have been developed.

A cavity dumper can be inserted in the Kerr-lens mode-locked Ti:sapphire laser resonator [83,84]. This allows the fs pulse to build up in a high Q cavity with essentially no outcoupling losses. When a certain energy is reached the cavity dumper (typically based on an acousto-optic modulator) is turned on, and the pulse is coupled out of the cavity. Repetition rates typically range from a few 100 kHz to a few MHz. Pulse energies of up to the 100-nJ level are possible.

Another method tries to exploit the inherent mode instability in solid-state lasers to show relaxation oscillations and self Q switching. In such regimes the envelope of the mode-locked pulse train is modulated. The Q-switched and mode-locked output can be stabilized by (weakly) amplitude modulating the pump at a frequency of several hundred kHz that is derived from the Q-switched envelope in a feedback loop [85].

A third technique is based on long laser cavities (up to tens of meters) resulting in low repetition rates of a few MHz. Careful cavity and dispersion design are necessary to avoid the multiple pulse lasing and the instabilities that are usually encountered with long cavities [86]. For example, 200-nJ, 30-fs pulses at a repetition rate of 11 MHz were obtained with a chirped mirror cavity and external pulse compression with prisms [87].

6.7.3. Cr:LiSAF, Cr:LiGAF, Cr:LiSGAF, and Alexandrite

The chromium ion has received substantial importance as a lasing medium. Ruby is produced by doping a sapphire host with Cr_2O_3. The ruby laser being a three-level system, requires high pump intensities to reach population inversion. It is a high gain, narrow bandwidth, laser, hence not suited for ultrashort pulse applications.

A broadband lasing medium is alexandrite, consisting of chromium doped chrysoberyl ($BeAl_2O_4:Cr^{3+}$). The alexandrite laser is generally flashlamp pumped (absorption bands from 380 to 630 nm) with a gain bandwidth ranging from 700 to 820 nm, and is therefore sometimes used as an amplifier (mostly regenerative amplifier) for pulses from Ti:sapphire lasers. It is one of those laser media in which the gain cross section increases with temperature, from $7 \cdot 10^{-21}$ cm^2 at 300°K to $2 \cdot 10^{-20}$ cm^2 at 475°K [72].

Of importance for femtosecond pulse generation are the Cr^{3+}:LiSrAlF$_6$ or Cr:LiSAF, Cr^{3+}:LiSrGaF$_6$ or Cr:LiSGAF and Cr^{3+}:LiCaAlF$_6$ or Cr:LiCAF lasers. These crystals have similar properties as shown in Table 6.3. The gain cross section is relatively low compared with other diode pumped laser crystals (30× less than that of Nd:YAG for example). The thermal conductivity is 10 × smaller

Table 6.3

Room temperature physical properties of Cr:LiSAF, Cr:LiSGAF, and Cr:LiCAF. The second-order dispersion of LiSAF is indicated for two different Cr doping concentrations. A_i, B_i, C_i, and D_i are the parameters of the Sellmeier formula $n_i^2 = A_i + B_i/(\lambda^2 - C_i) - D_i\lambda^2$, with $i = o$ (ordinary) or e (extraordinary), and λ expressed in μm.

Property	Cr:LiSAF	Cr:LiSGAF	Cr:LiCAF	Units	Ref.
Sellmeier coeff.					
A_o	1.95823	1.95733	1.91891		
A_e	1.95784	1.95580	1.91406		
B_o	0.00345	0.01306	0.00813	μm^2	
B_e	0.00324	0.00232	0.00985	μm^2	
C_o	0.02871	0.03834	0.04533	μm^2	
C_e	0.01023	0.03413	0.04130	μm^2	
D_o	0.05155	0.04741	0.02928	μm^{-2}	
D_e	0.02944	0.07423	0.01506	μm^{-2}	
n_o (850) nm	1.38730	1.38778	1.37900		
Nonlinear index	$3.3 \cdot 10^{-16}$	$3.5 \cdot 10^{-16}$	$3.7 \cdot 10^{-16}$	cm^2/W	[13]
Dispersion k''					
(850 nm, 0.8%)	210	207		fs^2/mm	[94,95]
Dispersion k''					
(850 nm, 3%)	230			fs^2/mm	[91]
Third-order					
dispersion k'''	1830	1340		fs^3/mm	[94,95]
Peak absorption	670	630		nm	
Peak gain at	850	850	763	nm	
cross section σ_e	$4.8 \cdot 10^{-20}$	$3.3 \cdot 10^{-20}$	$1.3 \cdot 10^{-20}$	cm^2	[93]
Fluorescence					
τ_F (300° K)	67	88	170	μs	[96]
$T_{1/2}$	69	75	255	°C	[88]
Expansion coeff.					
along a-axis	−10	0	3.6	10^{-6}/K	[93]
along c-axis	25	12	22	10^{-6}/K	[93]
c-axis thermal					
conductivity	3.3	3.6	5.14	W/mK	[94]
Thermal index					
dispersion dn/dT	−4.0		−4.6	10^{-6}/K	[94]

than for Ti:sapphire. Therefore, thin crystals are generally used for better cooling, which makes the mounting particularly delicate. The gain drops rapidly with temperature, because of increasing nonradiative decay. Stalder *et al.* [88] define a temperature $T_{1/2}$ at which the lifetime drops to half of the radiative decay time measured at low temperature. As shown in Table 6.3, this critical temperature is particularly low for Cr:LiSAF and Cr:LiSCAF (70°C) which, combined with

their poor thermal conductivity, makes these crystals unsuitable for high power applications. Cr:LiCAF is preferred to for other ions in applications such as regenerative amplifiers, because of its slightly larger saturation energy and better tolerance to a temperature increase.

The Cr^{3+}:$LiSrAlF_6$ is the most popular laser medium for low power, high efficiency operation. It is generally pumped by high brightness AlGaInP laser diodes. The emitting area section of a typical laser diode is rectangular, with a thickness of only a few microns, and a width equal to that of the diode. A "high brightness" diode is one for which the width does not exceed 200 μm. The shorter the diode stripe, the higher the brightness, and the lower the threshold for laser operation. Pump threshold powers as low as 2 mW have been obtained in diode pumped Cr^{3+}:$LiSrAlF_6$ lasers [89]. Mode-locked operation with 75-fs pulses was achieved with only 36 mW of pump power [90].

As can be seen from a comparison of Tables 6.2 and 6.3, the nonlinear index in LiSAF is significantly smaller than in Ti:sapphire. A careful design of the cavity including astigmatism compensation is required to have tighter focusing in the LiSAF crystal, leading to the same Kerr lensing than in a typical Ti:sapphire laser [90]. A pair of BK7 prisms (prism separation 360 mm) was found to be optimal for second- and third-order dispersion compensation, leading to pulses as short as 12 fs (200 MHz repetition rate) for a Cr:LiSAF laser, pumped by two diode lasers of 300 mW and 150 mW output power [95]. The average output power of the fs laser was 6 mW. Diode laser technology is the limiting factor in reaching high output powers. Indeed, 70 mW and 160 mW powers (14-fs pulse duration) are easily obtained by Kr-ion laser pumping of LiSAF and LiCAF, respectively [96]. One solution to alleviate the drawback of a relatively high brightness for higher power pump diodes, is to pump with a diode laser-pumped oscillator power amplifier system [97]. An output power of 50 mW was obtained with an absorbed pump power of 370 mW.

With chirped mirrors for dispersion compensation, the Cr:LiSAF laser should lend itself to compact structures at high repetition rate, although most lasers were operated at low (two 100 MHz [90–92,96,97]. The 12 fs Cr:LiSAF laser operating with a BK7 prism pair however had the shortest cavity, with a repetition rate of 300 MHz [95].

Because of the small nonlinear index n_2, it is often more convenient to use a single quantum well to initiate and maintain the mode-locking. Mode-locking with saturable absorber quantum wells was discussed in Section 6.6.

6.7.4. Cr:Forsterite and Cr:Cunyite Lasers

These two lasers use tetravalent chromium Cr^{4+} as a substitute for Si^{4+} in the host Mg_2SiO_4 (forsterite) [98,100] and as a substitute for Ge in the host

Table 6.4

Room-temperature physical properties of Cr:Forsterite and Cr:Colquiite lasers

Property	$Cr:Mg_2SiO_4$	$Cr:Ca_2GeO_4$	Units	Ref.
Nonlinear index	2×10^{-16}	1.5×10^{-14}	cm^2/W	[73,105]
Dispersion D^* at 1300 nm	145		fs^2/mm	[106]
Peak absorption α	670		nm	
Peak gain (1300 nm)	1.4	0.9	cm^{-20} cm^2	[72]
Fluorescence lifetime				[101]
τ_f	2.7	0.1	μs	[102,107]
Tuning range (nm)	1167	1330	nm	[72]
α	1348	1380	nm	
Thermal conductivity		0.03	W/cm/K	

Ca_2GeO_4 (colquiite) [101,102]. The properties of these two laser materials are compared in Table 6.4. Forsterite-based lasers have become important because they operate in the 1.3 μm range (1167 to 1345 nm) and can be pumped with Nd:YAG lasers. Amongst their other basic modes of diode pumping [103]. By careful intracavity dispersion compensation with a pair of SF58 prisms complemented by double-chirped mirrors, a pulse duration of 14 fs was obtained [104]. This laser, pumped by a Nd:YAG laser, had a threshold of 200 mW for cw operation and 4 W for mode-locked operation. 100 mW output power could be achieved with a pump power of 6 W.

The forsterite laser produces pulses short enough to create an octave spanning spectral bandwidth in fibers as discussed in Section 15.4.1.[4] A prismless compact ring cavity was designed with combination of chirped mirrors (GDD of -55 fs^2 from 1200 to 1415 nm) and Gires–Tournois interferometer mirrors (GDD of -200 fs^2 from 1200 to 1325 nm) as sketched in Figure 6.12. This laser, pumped by a 10 W fiber laser, combined short pulse output (28 fs) with a high repetition rate of 420 MHz [98].

6.7.5. YAG Lasers

The crystal $Y_3Al_5O_{12}$ or YAG is transparent from 300 nm to beyond 4 μm, optically isotropic, with a cubic lattice structure characteristic of garnets. It is one of the preferred laser hosts because of its good optical quality and high thermal conductivity. Some of the physical–optical properties are listed in Table 6.5. The two most important lasers using YAG as a host are Nd:YAG and Yb:YAG.

[4] Germanium doped silica fiber with a small effective area of 14 μm^2, nonlinear coefficient of 0.3 $W^{-1}km^{-1}$, zero dispersion near 1550 nm

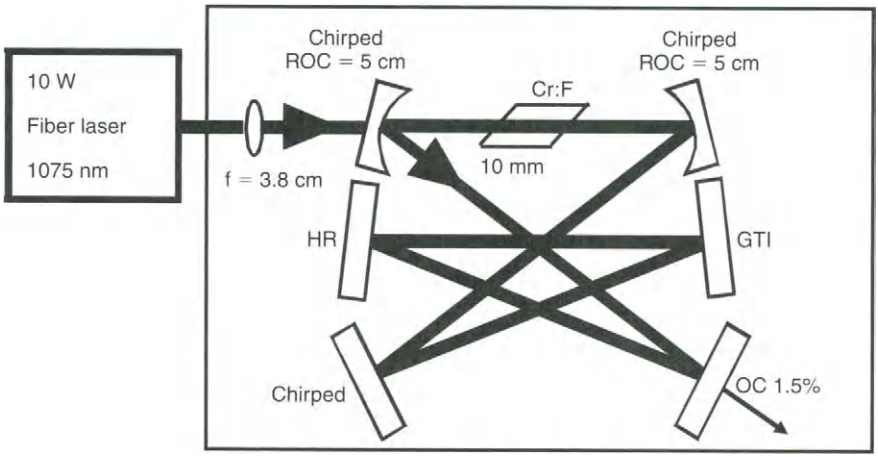

Figure 6.12 Compact ring cavity of a Cr:forsterite laser used in conjunction with HNLF fibers to generate an octave spanning continuum in the near IR. (Adapted from Thomann *et al.* [98].) The mirrors of 5 cm radius of curvature as well as the first folding mirror (HR) have chirped multilayer coatings. The second folding mirror is a Gires–Tournois Interferometer (GTI), the third one a standard high reflector, and the output coupler has a transmission of 1.5%.

Table 6.5

Room temperature physical properties of YAG. The second-order dispersion is calculated from the derivative of the Sellmeier equation: $n^2 = 1 + 2.2779\lambda_\ell^2/(\lambda_\ell^2 - 0.01142)$ with λ_ℓ in μm. The data are compiled from [70,72,104,108–110]

Property	YAG	Units
Index of refraction 1.064 μm	1.8169	
Index of refraction 1.030 μm	1.8173	
Dispersion (k'') at 1.064 μm	733	fs^2/cm
Dispersion (k'') at 1.030 μm	760	fs^2/cm
Nonlinear index	12.4	10^{-16} cm^2/W
Thermal expansion		
Ref. [100]	8.2	10^{-6} K^{-1}
Ref. [110]	7.7	10^{-6} K^{-1}
Ref. [111]	7.8	10^{-6} K^{-1}
Thermal conductivity	0.129	W cm^{-1} K^{-1}
dn/dT	8.9	10^{-6} K^{-1}

Nd:YAG

Typical doping concentrations of the Nd^{3+} ion (substitution of Y^{3+}) range from 0.2 to 1.4% (atomic). Larger doping degrades the optical quality of the crystal. Nd:YAG has been the workhorse industrial laser for several decades, because of its relatively high gain and broad absorption bands that makes it suitable for flashlamp pumping. It has a UV absorption band from 300 to 400 nm and absorption lines between 500 and 600 nm. It has also an absorption band at 808.6 nm which coincides with the emission of GaAlAs diode lasers. Being a four-level laser, Nd:YAG does not require as high a pump power to create an inversion as, for instance, the three level ruby laser or the Yb:YAG laser. The high gain is partly because of the narrow bandwidth of the fluorescence spectrum, limiting pulse durations to >10 ps. Despite this limitation, Nd:YAG has still a place as a source of (noisy) femtosecond pulses. Intracavity pulse compression by passive negative feedback (Section 6.5) yields mJ pulses as short as 8 ps directly from the oscillator [63,64]. Efficient conversion to the femtosecond range has been achieved either by intrinsic generation [111] or parametric oscillation [112,113]. The fundamentals of pulse compression associated with harmonic and parametric processes can be found in Sections 3.4.2 and 3.5.

Yb:YAG

Yb:YAG is a popular crystal for high average power, subpicosecond pulse generation. Up to 10 atomic percent of doping of the YAG crystal by Yb have been used. Table 6.6 compares some essential parameters of Nd:YAG and Yb:YAG. The main difference between the two crystals is that Yb:YAG is a quasi-three-level system, requiring large pump powers to overcome inversion. It does not have the broad absorption bands of Nd:YAG that would make it suitable for flashlamp pumping. The main advantage of Yb:YAG however is the small quantum defect.

Table 6.6

Comparison of Nd:YAG and Yb:YAG (data from [92,117])

Property	Nd:YAG	Yb:YAG	Units
Lasing wavelength	1064	1030	nm
Doping density (10 at.%)	1.38	1.38	10^{20} atoms/cm^3
Diode pump band	808.6	941	nm
Absorption bandwidth	2.5	18	nm
Emission cross section	28	2.1	10^{-20} cm^2
Emission bandwidth	0.45	9.0	nm
Fluorescence lifetime	230	951	μs

when pumped with InGaAs diode lasers at 942 nm. A small quantum defect implies that a minimum account of energy is dissipated in the crystal in the form of heat.

The combination of diode pumping (high wall plug efficiency), broad bandwidth and small quantum defect has spurred the development of short pulse, high average power Yb:YAG sources. The main problem to be overcome in developing high average output power sources is the removal of the heat produced by pump intensities of the order of kW/cm^2. Two solutions have been implemented, which led to pulse sources at 1.03 μm, subpicosecond pulse duration, and several tens of watts of average power:

1. A thin disk YbYAG laser [114] and
2. Laser rods with undoped endcaps.

The undoped endcaps allow for symmetrical heat extraction on either side of the beam waist. Typical average powers are between 20 and 70 W [21,115]. Quantum wells are generally used for mode-locking, with the exception of a 21 W, 124 MHz repetition laser using a variation of APML [71] (cf. Section 6.3).

In a thin-disk laser, the laser material has a thickness much smaller than the diameter of the pump and laser mode. One end side of the disk is coated for high reflectivity and is in direct contact with a heat sink. The resulting heat flow is longitudinal and nearly one-dimensional. Typical disks are 100 μm thick, for 10% doping with Yb. An average power of 60 W, for 810 fs pulses at a repetition rate of 34 MHz has been obtained [116].

5.7.6. Nd:YVO_4 and Nd:YLF

Both neodymium doped lithium yttrium fluoride (YLF) and vanadate (YVO_4) have gained importance as diode pumped lasers. The emission bandwidth is only slightly larger than that of Nd:YAG, hence the shortest pulse durations that are possible with these lasers are in the range of a few picoseconds (3 ps [118] to 5 ps [119] have been reported). The absorption bandwidth of Nd:vanadate is roughly 18 nm, as opposed to 2.5 nm for Nd:YAG, making it a preferred crystal for diode pumping.

Nd:YLF, like Alexandrite, is a long fluorescence medium (twice as long as Nd:YAG), hence an ideal storage medium for regenerative amplifiers. Its natural birefringence overwhelms the thermal stress induced birefringence, eliminating the depolarization problems of optically isotropic hosts like YAG. For example, a 15 W cw diode array was used to pump a Nd:YLF regenerative amplifier, amplifying at 1 kHz 15 ps, 20 μJ pulses to 0.5 mJ [120].

The main parameters of Nd:YLF and Nd:YVO_4 are summarized in Table 6.7.

Table 6.7

Properties of Nd:YVO_4 and Nd:YLF (data from [72,117]).*

Property	Nd:YVO_4	Nd:YLF	Units
Lasing wavelength	1064.3	1053 (σ)	nm
		1047 (π)	nm
Index of refraction		1.4481 (n_o)	
		1.4704 (n_e)	
Absorption (1% doping)			
σ	9		cm^{-1}
at	809	806	nm
π	31	4.5	cm^{-1}
at	809	797	nm
Absorption bandwidth	15.7		nm
Emission cross section	15		
σ	21	12	$10^{-20} cm^2$
π	76	18	$10^{-20} cm^2$
Gain bandwidth	0.96	1.3	nm
Fluorescence lifetime τ_F	90	480	μs
Thermal conductivity	0.05	0.06	$W\ cm^{-1}\ K^{-1}$
Thermal expansion in σ	8.5	−2	$10^{-6}\ K^{-1}$
Thermal expansion in π	3	−4.3	$10^{-6}\ K^{-1}$

*Parameters are listed for the radiation polarized parallel (π) and orthogonal (σ) to the optical axis of the crystal

6.8. SEMICONDUCTOR AND DYE LASERS

One of the main advantages of semiconductor and dye lasers is that they can be engineered to cover various regions of the spectrum. As opposed to the solid-state lasers of the previous sections, the semiconductor and dye lasers are characterized by a high gain cross section, which implies also a short upper state lifetime, typically shorter than the cavity round-trip time. Consequently, mode-locking through gain modulation can be effective.

6.8.1. Dye Lasers

Over the past 15 years fs dye lasers have been replaced by solid-state and fiber lasers. It was, however, the dye laser that started the revolution of sub 100-fs laser science and technology. In 1981 Fork *et al.* [121] introduced the colliding pulse mode-locked (CPM) dye laser that produced sub 100-fs pulses.

In this dye laser, the ring configuration allows two counter-propagating trains of pulses to evolve in the cavity [121].[5] The gain medium is an organic dye in solution (for instance, Rh 6G in ethylene glycol), which, pumped through a nozzle, forms a thin (≈ 100 μm) jet stream. Another flowing dye (for instance, diethyloxadicarbocyanine iodide, or DODCI, in ethylene glycol) acts as saturable absorber. The two counter-propagating pulses meet in the saturable absorber (this is the configuration of minimum losses).

A prism sequence (one, two, or four prisms) allows for the tuning of the resonator GVD. The pulse wavelength is determined by the spectral profiles of the gain and absorber dyes. Limited tuning is achieved by changing the dye concentration. Pulses shorter than 25 fs have been observed at output powers generally not exceeding 10 mW with cw pumping [122], and up to 60 mW with a pulsed (mode-locked argon laser) pump [123].

The palette of available organic dyes made it possible to cover practically all the visible to infrared with tunable and mode-locked sources. A table of gain absorber dye combinations used for passively mode-locked lasers can be found in Diels [124]. Hybrid mode-locking of dye lasers has extended the palette of wavelength hitherto available through passive mode-locking, making it possible to cover a broad spectral range spanning from extreme the visible from the UV to the near infrared. A list of dye combinations for hybrid mode-locking is given in Table 6.8. Except when noted, the laser cavity is linear, with the absorber and the gain media at opposite ends. Another frequently used configuration is noted "antiresonant ring." The saturable absorber jet is located near the pulse creating point of a small auxiliary cavity, in which the main pulse is split into two halves, which are recombined in a counting wave configuration in the absorber [116,125]. The ring laser appears only once in Table 6.8 [126], because of the difficulty of adjusting the cavity length independently of all other parameters.

Dye lasers have been particularly successful in the visible part of the spectrum, where virtually all wavelengths have been covered. The advantage of using an organic dye in a viscous solvent is that the flowing dye jet allows for extremely high pump power densities—in excess of 10 MW/cm^2—to be concentrated on the gain spot. The disadvantage of the dye laser lies also in the inconvenience associated with a circulating liquid system. One alternative for the liquid dye laser that conserves most of its characteristics is the dye doped, polymer nanoparticle gain medium. Significant progress has been made in developing a material with excellent optical quality [127,128]. These laser media have yet to be applied as a femtosecond source.

---

[5] The same ring configuration is sometimes used with a Titanium:sapphire gain medium, when a bidirectional mode of operation is sought.

Table 6.3

Femtosecond pulse generation by hybrid mode-locking of dye lasers pumped by cw argon-ion laser, except as indicated. (Adapted from [1284].) (ANB - antireasonant, p - pump laser)

Dye laser	Absorber[a]	λ_0 nm	Range	ν_{pump} fs	$\pi\lambda_0$ nm	Remarks
Disulfide fluorescein	RhB	570	570	450	560	
RB 110	RhB	560	560	290	560	
RB60	DODCI	574	611	300	606	
Rh6G	DODCI			180	620	Ring laser
Rh6G	DQDCI			90	590	ANB, cw
Rhen red 3	DQDCI			70	615	
RB 6	Cresidol 720	616	648	190	650	
9860101	DQDCI	650	650	30	570	Doubled
	DDCI	642	664	290	650	30 YAG p
Pyridine 1[b]	DDI			180	695	
Rhodamine 700	DQDCI	700	716	650	710	
Pyridine 2	DDI, DDTCI			240	733	
Rhodamine 700	IDTCI	730	781	650	730	
LDS-751	IDTCI	750	810	800		
Styryl 6	IDTCI		740	650		
Styryl 9[c]	LD 640[c]	650	680	65	650	Ring laser
Styryl 15	DeQTeC			220	974	

[a]See Appendix C for abbreviations.
[b]Solvent: propylene carbonate and ethylene glycol.
[c]In benzyl alcohol.

Miniature Dye Lasers

The long (compared to the geometrical length of a fs pulse) cavity of most mode-locked lasers serves an essential purpose where sequences of pulses—rather than a single pulse—is needed. Emission of a short pulse by the long resonator laser requires—as we have seen at the beginning of the previous chapter—a coherent superposition of the oscillating cavity modes with fixed phase relation. If, however, only a single pulse is needed, there is no need for more than one longitudinal mode within the gain profile. Ultrashort pulses are generated in small cavity lasers through resonator Q-switching and/or gain switching. Aside from gain bandwidth limitations, the pulse duration is set by the spectral width of the longitudinal mode, and hence the resonator lifetime. The latter in turn is limited by the resonator round-trip time $2L/c$. Ideally, the laser cavity should have a free spectral range $c/2L$ exceeding the gain bandwidth.

Two methods of short pulse generation that use either ultrashort cavities (Fabry–Perot dye cells of thickness in the micron range) or no traditional cavity at all (distributed feedback lasers) have successfully been developed for (but are not limited to) dye lasers.

In distributed feedback lasers two pump beams create a spatially modulated excitation that acts as a Bragg grating. This grating serves as the feedback (resonator) of the laser and is destroyed during the pulse evolution. This short cavity lifetime together with the small spatial extend of the gain volume can produce subps pulses whose frequency can be tuned by varying the grating period [129,130]. The tuning is determined by the overlap angle of the two pump beams.

In a typical "short cavity" laser, the wavelength is tuned by adjusting the thickness of the dye cell in a 3 to 3 μm range with a transducer bending slightly four back mirrors of the cavity [131]. With a roundtrip time of the order of only 10 fs, it is obvious that the pulse duration will not be longer than that of a ps pump pulse. As with the distributed feedback laser, the dynamics of pump depletion can result in pulses considerably shorter than the pump pulses. The basic operational principles of this laser can be found in Kurz *et al.* [132]. Technical details are given in Ohta *et al.* [131]. For example, using an excimer laser, Sorokin and Schäfer [130] produced 300 fs pulses, tunable from 400 to 960 nm, in a cascade of distributed feedback and short cavity dye lasers. After SPM and recompression, pulses as short as 30 fs in a spectral range from 423 to 630 nm were obtained [133].

Another type of miniature laser is the integrated circuit semiconductor laser, which will be described in the next section.

6.8.2. Semiconductor Lasers

Generalities

Semiconductor lasers are obvious candidates for fs pulse generation, because of their large bandwidth. A lower limit estimate for the bandwidth of a diode laser is $k_B T$ (where k_B is the Boltzmann constant and T the temperature), which at room temperature is (1/40) eV, corresponding to a 15-nm bandwidth at 850 nm, or a minimum pulse duration of 50 fs. The main advantage of semiconductor lasers is that they can be directly electrically pumped. In the conventional diode laser, the gain medium is a narrow inverted region of a *p–n* junction. We refer to a publication of Basov [134] for a detailed tutorial review on short pulse generation with diode lasers. We will mainly concentrate here on problems associated with fs pulse generation in external and internal cavity (integrated) semiconductor lasers. The main technical challenges associated with laser diodes result from the small cross section of the active region (typically 1 μm by tens of μm), the

large index of refraction of the material ($2.5 < n < 3.5$, typically) and the large nonlinearities of semiconductors.

The cleaved faces of a laser diode form a Fabry–Perot resonator with a mode spacing of the order of 1.5 THz. Two options are thus conceivable for the development of fs lasers: integrate the diode with a waveguide in the semiconductor, to construct fs lasers of THz repetition rates, or attempt to "neutralize" the Fabry–Perot effect of the chip, and couple the gain medium to an external cavity. We will consider first the latter approach.

External Cavity

Because of the high refractive index of the semiconductor, it is difficult to eliminate the Fabry–Perot resonances of the short resonator made by the cleaved faces of the crystal. Antireflection coatings have to be of exceptionally high quality. Even though reflectivities as low as 10^{-4} can be achieved, a good quality antireflection coating with a high optical damage threshold remains a technical challenge. A solution to this problem is the angled stripe semiconductor laser [135], which has the gain channel cutting an angle of typically 5° with the normal to the facets (Figure 6.13). Because of that angle, the Fabry–Perot resonance of the crystal can easily be decoupled from that of the external cavity. A standard antireflection coating applied to the semiconductor chip is sufficient to operate the laser with an external cavity.

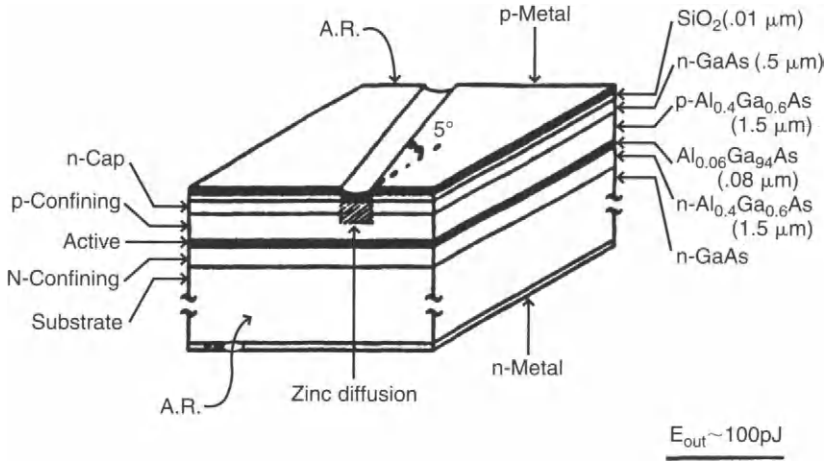

Figure 6.13 Structure of an angled stripe semiconductor laser. (Adapted from [135].)

Femtosecond pulse operation in a semiconductor laser with an external cavity is similar to that of a dye laser. The laser can be cw pumped, as in Delfyett *et al.* [136]. Best results so far were obtained in hybrid operation, using radio frequency current modulation for gain modulation (synchronous pumping), and a saturable absorber. The low intracavity power of the external cavity semiconductor laser—as compared to the dye laser—makes the use of conventional saturable absorbers (i.e., dyes, bulk semiconductors) impractical. It has been necessary to develop absorbing structures with a low saturation energy density. These are the MQW absorbers, which were analyzed in Section 4.6. The laser diode is modulated at the cavity round-trip frequency (0.5 W RF power applied via a bias tee [68]). Modulation of the index of refraction is associated with the gain depletion and the saturation of the MQW. Because the gain depletion results in an increase of the index, a negative dispersion line appears appropriate. Bandwidth-limited operation is difficult to achieve directly from a mode-locked semiconductor laser. An external dispersive line with gratings resulted in pulse durations of 200 fs [137].

The exact phase modulation mechanism of that laser is complex. The index of refraction of the diode is a function of temperature and that carrier density, which itself is a function of current, bias, light intensity, etc. As with other high gain solid-state lasers, changes in the pulse parameters can be as large as 50% from one element to the next [68].

Current Modulation To take full advantage of the fast filtering of the gain in a semiconductor laser, one should have a circuit that drives short current pulses into the diode. As mentioned above, a feedback technique—generally referred to as regenerative feedback—can be used to produce a sine wave driving current exactly at the cavity repetition rate. The circuit consists essentially in a phase locked loop, synchronized by the signal of a photodiode monitoring the mode beat note of the laser, and a passive filter at the cavity round-trip frequency. A comb generator can be used to transform the sine wave in a train of short electrical pulses. A comb generator is a passive device which produces, in the frequency domain, a "comb" of higher harmonics which are integral multiples of the input frequency. As we had seen in the Introduction of Chapter 3, to a regular frequency comb corresponds a periodic signal in the time domain. This periodic signal can correspond to short pulses, if—and only if—the teeth of the comb are in phase. Commercial comb generators are generally constructed to create higher harmonics, without being optimized for creating a phased comb. Therefore a selection should be made among these devices to find a generator with good temporal properties (shortest pulse generation).

To allow for the injection of a short current pulse into the laser diode, the latter should be designed with minimal capacitance. To this effect, the p and n

contacts of the angle striped diode of Fig. 6.13 should not cover the whole area of the strip, but be limited to a narrow stripe which follows the gain line.

Integrated Devices

Instead of trying to couple the semiconductor chip to a external laser cavity, one can integrate the semiconductor into a waveguide cavity. Such devices ranging in length from 0.25 mm to 2 mm have been constructed and demonstrated for example by Chen and Wang [138]. The end mirrors of the cavity are—as in a conventional diode laser—the cleaved faces of the crystal (InP) used as substrate. Wave guiding is provided by graded index confining InGaAsP layers. Gain and saturable absorber media consist of MQWs of InGaAs. The amount of gain and saturable absorption is controlled by the current flowing through these parts of the device (reverse bias for the absorber). As shown in the sketch of Figure 6.14, the saturable absorber is located at the center of symmetry of the device, sandwiched between two gain regions. This configuration is analogous in idea to the ring dye laser, in which the two counter-propagating pulses meet coherently in the absorber jet. In the case of this symmetric linear cavity, the laser operation of mid-beam lasers will correspond to two circulating pulses overlapping as standing waves in the saturable absorber.

These devices are pumped continuously and are thus the solid-state equivalent of the passively mode-locked dye lasers. The laser parameters can, however, be significantly different. Although the average output power is only slightly inferior to that of a dye laser (1 mW), at the much higher repetition rate (up to 350 GHz), the pulse energy is only in the fW range! For these extended cavity lengths, there are only a handful of modes contained by the gain bandwidth.

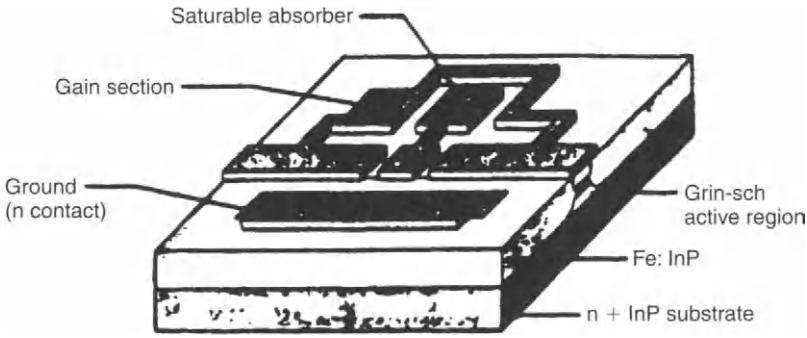

Figure 6.14 Layout of an integrated semiconductor laser. (Adapted from [138].)

Semi-Integrated Circuit Fe Lasers

Total integration as shown above results in a high duty cycle, at the expense of a lower energy per pulse. On can seek a compromise between the discrete element semiconductor laser and the total integrated laser. For instance, the integration of the gain and saturable absorber of the integrated laser of Chen and Wang [138] can be maintained in a single element coupled to an external cavity. Such a design has been successfully tested by Lin and Tang [139]. The absorber consists of a 10 μm island in middle of the gain region, on it an electrical contact, isolated from the gain structure by two 10-μm shallow etched regions (without any electrical contact). The absorption—as in the case of the totally integrated laser—can be controlled through the bias potential of the central contact. To prevent lasing action of the 330-μm long gain medium, the end facets—after cleavage—are etched (chemically assisted ion beam etching) at 10° from the cleaved plane. The autocorrelation of the laser pulses from such a structure had a width of approximately 700 fs [139].

6.9. FIBER LASERS

6.9.1. Introduction

In most lasers discussed so far, the radiation in a fiber propagating wave in the gain or other elements of the cavity. The gain length is limited by the volume that can be pumped. The length of a nonlinear interaction is also limited by the Rayleigh range (z_0). By confining the wave in a wave guide, it is possible to have arbitrarily long gain media and nonlinear effects over arbitrarily long distances. A fiber is an ideal wave guide for this purpose. Its losses can be as small as a few dB/km. Yet the pulse configuration is such that substantial phase modulation can be achieved over distances ranging from cm to m. The fiber is particularly attractive in the wavelength range of negative dispersion (beyond 1.3 μm), because the combination of phase modulation and dispersion can lead to pulse (soliton) compression (see Chapter II). The gain can be provided by Stimulated Raman Scattering (SRS) in the fiber material. Such "Raman soliton lasers" are reviewed in the next subsection. In the following subsections, we will consider the case of doped fibers, where the gain medium is of the same type as in conventional glass lasers.

Over the past 20 years ultrafast fiber lasers have matured dramatically. Compact, turn key systems are available commercially today and can deliver tens of mW of average power at pulse durations of the order of 100 fs. With amplification the micro Joule level is accessible. These lasers have applications

as self-standing units or as compact seed sources for high-power fs amplifier systems.

6.9.2. Raman Soliton Fiber Lasers

SRS is associated with intense pulse propagation in optical fibers. A review of this topic can be found in Rudolph and Wilhelmi [140] for example. The broad Raman gain profile for the Stokes pulse extends up to the frequency of the pump pulse. An overlap region exists because of the broad pump pulse spectrum. The lower frequency components of the pulse can experience gain at the expense of attenuation of the higher frequency components. In addition, the amplification of spontaneously scattered light is possible. Either process leads to the formation of a Stokes pulse which separates from the pump pulse after the walk-off distance because of GVD. These processes can be utilized for femtosecond Raman soliton generation in fibers and fiber lasers [141–143]. An implementation of this idea is shown in Figure 6.15. The pulses from a cw mode-locked Nd:YAG laser

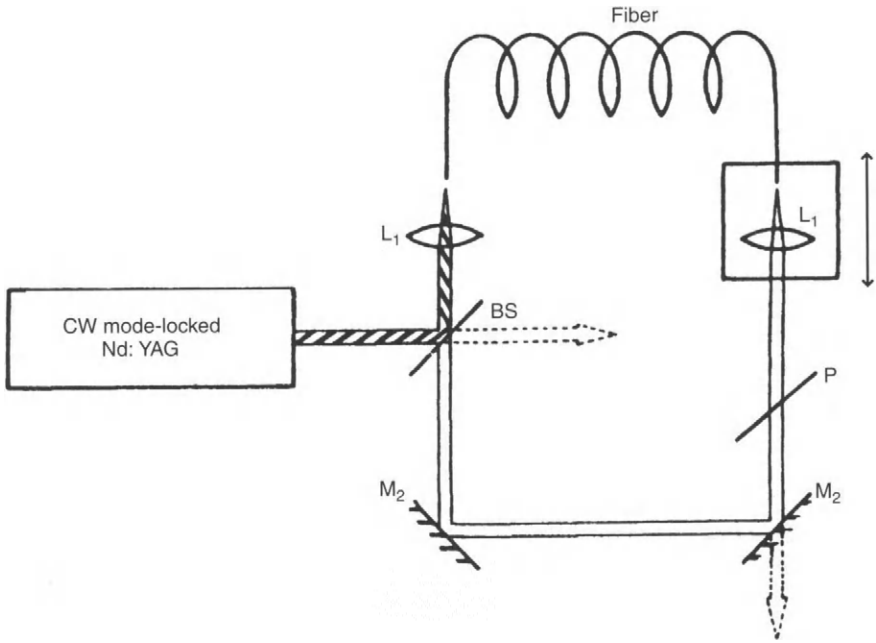

Figure 6.15 Experimental configuration of a synchronously pumped fiber ring Raman laser. (Adapted from Gouveia-Neto [143].)

(100 MHz, 100 ps, 1.32 μm) are coupled through a beam splitter BS into a ring laser containing an optical fiber. The fiber was tailored to have a negative dispersion for $\lambda_2 > 1.46$ μm. While traveling through the fiber the pump pulses at 1.319 nm produce Stokes pulses at $\lambda_1 = 1.41$ μm. This first Stokes pulse in turn can act as pump source for the generation of a second Stokes pulse ($\lambda_2 = 1.495$ μm), which is in the dispersion region that enables soliton formation. Of course, for efficient synchronous pumping, the length of the ring laser had to be matched to the repetition rate of the pump. Second Stokes pulses as short as 260 fs were obtained.

6.9.3. Doped Fiber Lasers

Fibers can be doped with any of the rare earth ions used for glass lasers. Whether pumped through the fiber end, or transversely, these amplifying media can have an exceptionally large optical thickness ($\alpha_p = \sigma_p N_2 \gg 1$). An initial demonstration of this device was made by Snitzer [144,145]. Passively mode locked rare earth doped fiber lasers later since evolved into compact, convenient, and reliable sources of pulses shorter than 100 fs. The gain media generally used are Nd^{3+} operating at 1050 nm and Er^{3+} at 1550 nm. The erbium doped fiber is sometimes codoped with ytterbium, because of the broad absorption band of the latter centered at ≈ 980 nm and extending well beyond 1000 nm. Pump light at 1.06 μm can be absorbed by ytterbium, which then transfers the absorbed energy to the Er ions. High gain and signal powers can thus be obtained by using, for example, diode laser pumped miniature Nd:YAG lasers.

Because of the high gain in a typical fiber laser, it may include bulk optic components, e.g., mirror cavities, dispersion compensating prisms, or saturable absorbers. Obviously, the preferred configuration is that of an all-fiber laser, using a variety of pigtailed optical components and fused spectral couplers for output and pumping.

As compared to conventional solid-state lasers, fibers have the advantage of a large surface to volume ratio (hence efficient cooling is possible). The specific advantages of the single mode fiber geometry over bulk solid-state (rare earth) media for mode-locking are:

- Efficient conversion of the pump to the signal wavelength. Erbium, for example, is a three-level system and the tight mode confinement of the pump in a fiber allows for efficient depopulation of the ground state and thus high efficiency.
- Nonradiative ion–ion transitions that deplete the upper laser level are minimized. Such interactions are especially egregious in silica because of its high phonon energy, and because the ultraviolet dopants do not mix

well into the quartzlike silica matrix, tending instead to form strongly interacting clusters at the high concentrations necessary for practical bulk glass lasers [146]. The confinement of both the laser and pump modes allows the gain dopant to be distributed along greater lengths of fiber at lower concentration, obviating the need for high concentrations and so eliminating the interactions cited previously.

- Diode laser pumping is practicable (due in large part to the previous two points). Single mode laser diodes have been developed at 980 nm and 1480 nm for erbium fiber amplifiers in telecommunications applications. The four-level structure of neodymium allows for pumping even by multimode lasers, such as high-power laser diode arrays, by using fibers designed to guide the pump light in the cladding [147].
- Tight mode confinement and long propagation lengths maximize the SPM by the weak nonlinear index of silica ($\bar{n}_2 = 3 \cdot 10^{-16}$ cm^2/W).
- The dispersion k'' of fibers (including the sign) can be tailored to the application.

One drawback of the fiber laser is that the confinement limits the pulse energies that can be produced. In bulk-solid state lasers, the problem of material damage can be overcome by beam expansion.

A number of techniques have been developed to mode-lock fiber lasers. The most successful methods are

1. nonlinear polarization rotation [148],
2. nonlinear loop mirrors [149],
3. mode-locking with semiconductor saturable absorbers [150].

Femtosecond pulse output with durations of 100 fs and below has been observed with a variety of gain media—Nd, Yb, Er, Er/Yb, Pr, and Tm. For a detailed overview on mode lasers we refer the reader to a review paper by Fermann *et al.* [151].

6.9.4. Mode-Locking through Polarization Rotation

Because of its central importance in today's fs laser lasers we will describe one of the mode-locking techniques—nonlinear polarization rotation—in more detail. As explained in Section 5.4.2 nonlinear polarization rotation in combination with polarizers can act as a fast saturable absorber, cf. Eq. (5.84). In a fiber laser using nonlinear polarization rotation, the differential accumulated phase yields an intensity-dependent rotation of polarization across the pulse. This polarization

state is then converted into an intensity-dependent transmission by inserting a polarizer at the output of the birefringent element, oriented, for example, to transmit the high intensity central portion of the pulse and reject the wings. This approach is the fiber equivalent of the Kerr lens mode-locked Ti:sapphire laser. Pulses as short as 36 fs have been obtained from an Yb fiber laser that used nonlinear polarization rotation [152], to name just one example.

A standard single mode fiber serves as nonlinear element. Such a fiber has generally a small birefringence. The degree of birefringence is defined by the parameter

$$B = \frac{|k_x - k_y|}{2\pi/\lambda_c} = |n_x - n_y|, \tag{6.9}$$

where n_x and n_y are the effective refractive indices for the two orthogonal polarization states. For a given value of B, the power between the two modes (field components along $\hat{x}$ and $\hat{y}$) is exchanged periodically, with a period ℓ_B called the "beat length" given by [153]:

$$\ell_B = \frac{\lambda_c}{B}. \tag{6.10}$$

The axis with the larger mode index is called the slow axis. In a typical single mode fiber, the beat length is around 2 to 10 m at $\lambda = 1.55$ μm [154]. As shown by Stolen [155], nonlinear polarization effects can be observed at reasonably low power in weakly birefringent fibers (as opposed to polarization preserving fibers).

In a typical fiber ring cavity a fiber polarization controller produces an elliptical polarization, whose major axis makes a small angle θ with the slow axis of the portion of fiber that follows. As shown in Section 5.A.2 the induced phase difference between two orthogonal polarization components depends on the propagation distance z and the pulse intensity. It can be adjusted such that after a distance ℓ_B the polarization becomes linear. A polarizer can be used to reject the loss for the lower intensities as compared to the higher intensities, as sketched in Figure 6.16.

We have derived in Section 5.A.2 the essential equations relating to nonlinear polarization rotation. To describe a fiber laser we need to track the evolution of two polarization components. This can conveniently be done using a column vector for the electric field in a certain pulse in the cavity

$$\begin{pmatrix} \mathcal{E}_x \\ \mathcal{E}_y \end{pmatrix}, \tag{6.11}$$

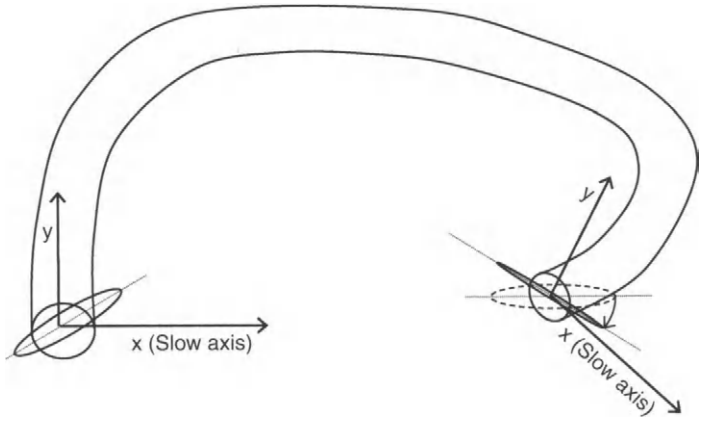

Figure 6.16 Sketch of the nonlinear polarization rotation in a fiber. The elliptically polarized input can be converted into linearly polarized light at the peak of the pulse for example.

and 2×2 matrices ($\mathcal{M}$) for the resonator elements [156,157]. The effect of the nonlinear birefringent fiber of length L is the combination of a linear propagation problem and nonlinear phase modulation. The resulting matrix is thus a product of two matrices, and the field vector is given by:

$$\begin{pmatrix} \tilde{\mathcal{E}}_x(L) \\ \tilde{\mathcal{E}}_y(L) \end{pmatrix} = \begin{pmatrix} e^{-i\Phi_{NL,x}} & 0 \\ 0 & e^{-i\Phi_{NL,y}} \end{pmatrix} \cdot \begin{pmatrix} e^{-ik_x L} & 0 \\ 0 & e^{-ik_y L} \end{pmatrix} \cdot \begin{pmatrix} \tilde{\mathcal{E}}_x(0) \\ \tilde{\mathcal{E}}_y(0) \end{pmatrix}$$

$$= \begin{pmatrix} e^{-i\Phi_x} & 0 \\ 0 & e^{-i\Phi_y} \end{pmatrix} \cdot \begin{pmatrix} \tilde{\mathcal{E}}_x(0) \\ \tilde{\mathcal{E}}_y(0) \end{pmatrix}, \tag{6.12}$$

where

$$\Phi_{x,y} = \frac{2\pi n_2 L}{\lambda_\ell} \left[|\tilde{\mathcal{E}}_{x,y}|^2 + \frac{2}{3} |\tilde{\mathcal{E}}_{y,x}|^2 \right] - \frac{2\pi n_{x,y} L}{\lambda_\ell}.$$

We have used here the same approximations for the nonlinear phase as in Section 5.4.2. The linear propagation constants $k_{x,y} = \omega_\ell n_{x,y}/c$. Matrices of common polarizing elements like wave plates and polarizers known from Jones calculus can easily be incorporated into this analysis.

Other components of the round-trip model like gain, saturable absorption, mirrors, etc., usually do not distinguish between the two polarization components. The transfer functions $\mathcal{T}$ are those introduced in Chapter 5. For implementing

these elements in a way consistent with the matrix approach we define a transfer matrix

$$(M) = T\begin{pmatrix} 1 & 0 \\ 0 & 1 \end{pmatrix}. \tag{6.13}$$

Fiber lasers have typically high gain and losses. The laser operates in a regime of strong saturation, with pulses much shorter than the energy relaxation time of the lasing transition. The gain saturation is generally sufficiently bandwidth for pulse amplification because of saturation to be negligible. Therefore the T factor in the transfer matrix describing gain is real and can be obtained from Eq. (3.55):

$$T_g = \left[\frac{e^{W_{sat}/W_s}}{e^{W_{sat}/W_s} - 1 + e^{W_0/W_s}}\right]^{1/2}. \tag{6.14}$$

An alternative approach is to consider the fiber laser as a continuous medium, which leads to a coupled system of differential equations for the components $\bar{E}_x$ and $\bar{E}_y$. This is essentially a two-field component extension of Eq. (3.190) without the inverse differential operators. We refer to the literature for a derivation of this system of equations and for their application to the modeling of a mode-locked fiber ring laser using nonlinear polarization rotation, Chang and Chi [137], Chi *et al.* [138], Agrawal [139], and Spaulding *et al.* [140].

6.9.5. Figure-Eight Laser

A widely studied fiber laser implementation of the nonlinear mirror is the figure-eight laser [144], so named for the schematic layout of its components (Figure 6.17), with a nonlinear amplifying loop mirror [161]. In the example shown in Fig. 6.17, the laser consists of a nonlinear amplifying mirror (left loop) and an optical isolator with outcoupler (right loop). The two loops of the "figure-eight" are connected by a 50% beam splitter.

Let us follow a pulse that propagates counterclockwise in the right loop through the isolator (optical diode), through a polarization controller (to compensate for the natural birefringence of the fiber) and a 20% output coupler. The remaining part of the circulating pulse is equally split into the two directions of the left loop (nonlinear mirror). The counter-propagating pulses experience the same gain in the Er-doped fiber section of about 2 to 3 dB. The switching fiber introduces a phase shift through SPM. Being amplified before entering this fiber section, the counterclockwise circulating pulse experiences a larger phase shift than its replica propagating in the opposite direction. The two pulses arrive simultaneously at the fiber splitter and recombine. The variation of the

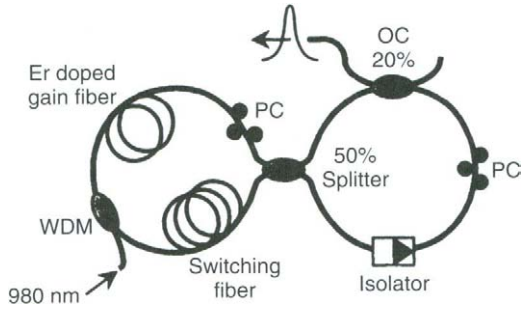

Figure 6.17 Schematic representation of the figure eight laser. The pump radiation at 980 nm is injected via the directional coupler WDM in the gain fiber (erbium doped). (Adapted from Duling [144].)

accumulated differential phase across the combined pulse will create different parts of the pulse injected clockwise and counterclockwise into the left loop. From the point of view of the counterpropagating pulse in the right loop, the left loop acts as a nonlinear mirror whose reflection varies sinusoidally as a function of intensity. Thus, the loop mirror behaves as a fast saturable absorber from low intensity to intensities corresponding to the first transmission maximum.

Fiber lasers operating on the 1050 nm transition of Nd^{3+} in silica require bulk optic elements (prism sequences) for compensating the substantial normal dispersion (30 ps/nm · km) of the gain fiber at the operating wavelength, and so are generally constructed as a bulk optic external cavity around the gain fiber. Passive mode-locking is obtained via nonlinear polarization rotation in the gain fiber, and the Brewster angled prisms serve as the polarizer. Pulses as short as 100 fs have been demonstrated [162].

Femtosecond fiber lasers operating in the 1530–1570 nm gain band of erbium are of obvious interest for their potential application in telecommunications. This wavelength range is in the low loss window of silica fibers, and such a source is obviously compatible with erbium fiber amplifiers. Of particular interest also is the anomalous dispersion exhibited by silica at this wavelength. The precise value of the dispersion may be tailored through the exact fiber design. This implies that a mode-locked laser with Er gain may be constructed entirely from fibers, with no need for dispersion compensating prisms as in the Nd fiber lasers or other solid-state sources. Indeed, subpicosecond erbium lasers have been demonstrated with all-fiber figure-eight, linear, and ring cavities, using both nonlinear mirrors and nonlinear polarization rotation. In addition, systems using semiconductor saturable absorbers have been demonstrated.

While soliton-like models have been used to describe a number of ultrafast laser systems as discussed in Chapter 5, the nonlinear dynamics of soliton propagation plays a more direct role in the erbium fiber laser than it does in any other. The generated pulses are typically transform limited with a sech^2 intensity profile—the shape expected from the soliton solution of the nonlinear Schrödinger equation. The average intracavity energy per pulse corresponds reasonably well to the energy of a soliton of the same length propagating in fiber with dispersion equal to the average cavity dispersion.

It has been demonstrated that the minimum pulse length obtainable in erbium fiber lasers is approximately proportional to the total dispersion inside the cavity [163]. This is to some degree surprising: As the pulse propagation is soliton-like, the fiber dispersion is continuously balanced by the SPM of the fiber. In principle, solitons of any length will form as long as the amplitude of the input pulse exceeds the threshold value of Eq. (3.55) (cf. soliton description in Chapter 3). However, the coupling of energy into the dispersive wave increases exponentially as the pulse shortens, thus limiting the minimum obtainable pulse width [164]. This loss becomes important only when the cavity length is of the order of the characteristic soliton length defined in Eq. (3.37). This is also why dispersive wave dynamics do not play an important role in other mode-locked lasers, that can be described by a soliton model. In such systems the soliton length corresponds to many cavity round-trips, much longer than the cavity lifetime of the dispersive wave. To obtain short pulses, then, it is necessary to minimize the total cavity dispersion, either by using dispersion shifted fiber components, or short cavities, or by including lengths of dispersion compensating fiber specially designed to have normal dispersion at 1550 nm. Pulse widths of less than 100 fs [165] have been achieved. With such short pulses, third-order dispersion plays an important role in limiting the pulse width and may impose a nonlinear chirp on the pulse [166].

BIBLIOGRAPHY

[1] R. Ell, U. Morgner, F. X. Kärtner, J. G. Fujimoto, E. P. Ippen, V. Scheuer, G. Angelow, T. Tschudi, M. J. Lederer, A. Boiko, and B. Luther-Davies. Generation of 5-fs pulses and octave-spanning spectra directly from a Ti:sapphire laser. *Optics Letters*, 26:373–375, 2001.

[2] D. E. Spence, J. M. Evans, W. E. Sleat, and W. Sibbett. Regeneratively initiated self-mode-locked Ti:sapphire laser. *Optics Letters*, 16:1762–1764, 1991.

[3] E. W. Van Stryland. The effect of pulse to pulse variation on ultrashort pulsewidth measurements. *Optics Communications*, 31:93–96, 1979.

[4] J.-C. Diels, J. J. Fontaine, I. C. McMichael, and F. Simoni. Control and measurement of ultrashort pulse shapes (in amplitude and phase) with femtosecond accuracy. *Applied Optics*, 24:1270–1282, 1985.

[5] G. H. C. New and J. M. Catherall. Advances in the theory of mode-locking by synchronous pumping. In G. R. Fleming and A. E. Siegman, Eds., *Ultrafast Phenomena V*. Springer-Verlag, Berlin, Germany, 1986, pp. 24–26.

[6] U. Stamm. Numerical analysis of pulse generation in synchronously mode locked cw dye lasers. *Applied Physics B*, B45:101–108, 1988.

[7] V. A. Nekhaenko, S. M. Pershin, and A. A. Podshivalov. Synchronously pumped tunable picosecond lasers (review). *Soviet Journal of Quantum Electronics*, 16:299–315, 1986.

[8] N. J. Frigo, H. Mahr, and T. Daly. A study of forced mode locked cw dye lasers. *IEEE Journal of Quantum Electronics*, QE-13:1134, 1977.

[9] A. M. Johnson and W. M. Simpson. Tunable femtosecond dye laser synchronously pumped by the compressed second harmonic of Nd:YAG. *Journal of the Optical Society of America B*, B2:619–625, 1985.

[10] G. Angel, R. Gagel, and A. Laubereau. Generation of femtosecond pulses by a hybrid laser system. *Optics Communications*, 63:259–263, 1987.

[11] L. Turi and F. Krausz. Amplitude modulation mode locking of lasers with regenerative feedback. *Applied Physics Letters*, 58:810, 1991.

[12] J. M. Catherall and G. H. C. New. Role of spontaneous emission in the dynamics of mode-locking by synchronous pumping. *IEEE Journal of Quantum Electronics*, QE-22:1593, 1986.

[13] D. S. Peter, P. Beaud, W. Hodel, and H. P. Weber. Passive stabilization of a synchronously pumped mode-locked dye laser with the use of a modified [illegible]. *Optics Letters*, 16:405, 1991.

[14] J. P. Ryan, L. S. Goldberg, and D. J. Bradley. Comparison of synchronous pumping and passive mode-locking cw dye lasers for the generation of picosecond and subpicosecond light pulses. *Optics Communications*, 27:127–133, 1978.

[15] B. Couillaud, V. Fossati-Bellani, and G. Mitchel. Ultrashort pulse spectroscopy and applications. In *SPIE Proceedings*, volume 533, Springer-Verlag, Berlin, Germany, 1985, p. 46.

[16] N. Jamasbi, J.-C. Diels, and L. Sarger. Study of a linear femtosecond laser in passive and hybrid operation. *Journal of Modern Optics*, 35:1891–1906, 1988.

[17] V. Petrov, W. Rudolph, U. Stamm, and B. Wilhelmi. Limits of ultrashort pulse generation in cw mode-locked dye lasers. *Physical Review A*, 40:1474–1483, 1989.

[18] L. C. Foster, M. D. Ewy, and C. B. Crumly. Laser mode locking by an external Doppler cell. *Applied Physics Letters*, 6:6–8, 1965.

[19] R. W. Dunn, A. T. Hendow, J. G. Small, and E. Stijns. Gas laser mode-locking using an external acoustooptic modulator with a proposed application to passive ring gyroscopes. *Applied Optics*, 21:3984–3986, 1982.

[20] K. J. Blow and D. Wood. Mode-locked lasers with nonlinear external cavities. *Journal of the Optical Society of America B*, 5:629–632, 1988.

[21] K. J. Blow and B. P. Nelson. Improved mode locking of an F-center laser with a nonlinear nonsoliton external cavity. *Optics Letters*, 13:1026–1028, 1988.

[22] P. N. Kean, X. Zhu, D. W. Crust, R. S. Grant, N. Langford, and W. Sibbett. Enhanced mode locking of color-center lasers by coupled-cavity feedback control. *Optics Letters*, 14:39, 1989.

[23] J. Mark, L. Y. Liu, K. L. Hall, H. A. Haus, and E. P. Ippen. Femtosecond laser pumped by a frequency-doubled diode-pumped Nd:YLF laser. *Optics Letters*, 14:48–50, 1989.

[24] C. P. Yakymyshyn, J. F. Pinto, and C. R. Pollock. Additive-pulse mode-locked NaCl:OH laser. *Optics Letters*, 14:621–623, 1989.

[25] P. M. French, J. A. R. Williams, and J. R. Taylor. Femtosecond pulse generation from a titanium-doped sapphire laser using nonlinear external cavity feedback. *Optics Letters*, 14:686, 1989.

[26] J. Goodberlet, J. Wang, J. G. Fujimoto, and P. A. Schulz. Femtosecond passively mode-locked Ti:sapphire laser with a nonlinear external cavity. *Optics Letters*, 14:1125–1127, 1989.

[27] J. Goodberlet, J. Jacobson, J. G. Fujimoto, P. A. Schulz, and T. Y. Fan. Self-starting additive-pulse mode-locked diode-pumped Nd:YAG laser. *Optics Letters*, 15:504–506, 1990.

[28] L. Y. Liu, J. M. Huxley, E. P. Ippen, and H. A. Haus. Self-starting additive-pulse mode locking of a Nd:YAG laser. *Optics Letters*, 15:553–555, 1990.

[29] J. M. Liu and J. K. Chee. Passive mode locking of a cw Nd:YLF laser with a nonlinear external coupled cavity. *Optics Letters*, 15:685, 1990.

[30] J. Goodberlet, J. Jacobson, J. G. Fujimoto, and P. A. Schulz. Ultrashort pulse generation with additive pulse modelocking in solid state lasers: Ti : Al_2O_3, diode pumped Nd:YAG and Nd:YLF. In C. B. Harris, E. P. Ippen, G. A. Mourou, and A. H. Zewail, Eds., *Ultrafast Phenomena VII*, Springer-Verlag, Berlin, Germany, 1990, p. 11.

[31] P. Krumins, C. Spielmann, T. Brabec, E. Wintner, and A. J. Schmidt. Subpicosecond pulse generation from a Nd:glass laser using a nonlinear external cavity. *Optics Letters*, 15:737–739, 1990.

[32] W. Sibbett. Hybrid and passive mode-locking in coupled-cavity lasers. In C. B. Harris, E. P. Ippen, G. A. Mourou, and A. H. Zewail, Eds., *Ultrafast Phenomena VII*, Springer-Verlag, Berlin, Germany, 1990, p. 2–7.

[33] E. P. Ippen, H. A. Haus, and L. Y. Liu. Additive pulse mode locking. *Journal of the Optical Society of America B*, 6:1736, 1989.

[34] L. F. Mollenauer and R. H. Stolen. The soliton laser. *Optics Letters*, 9:13, 1984.

[35] U. Keller, G. W. 'tHooft, W. H. Knox, and J. E. Cunningham. Femtosecond pulses from a continuously self-starting passively mode-locked Ti:sapphire laser. *Optics Letters*, 16:1022–1024, 1991.

[36] M. Sheik-Bahae, D. J. Hagan, and E. W. Van Stryland. Dispersion and band-gap scaling of the electronic Kerr effect in solids associated with two-photon absorption. *Physical Review Letters*, 65:96–99, 1990.

[37] M. Sheik-Bahae, D. C. Hutchings, D. J. Hagan, and E. W. Van Stryland. Dispersion of bound electronic nonlinear refraction in solids. *IEEE Journal of Quantum Electronics*, QE-27:1296–1309, 1991.

[38] G. Cerullo, M. B. Danailov, S. De Silvestri, P. Laporta, V. Magni, D. Segala, and S. Taccheo. Nonlinear mirror mode-locking of a cw Nd:YAG laser. *Applied Physics Letters*, 65:2392–2394, 1994.

[39] M. B. Danailov, G. Cerullo, V. Magni, D. Segala, and S. De Silvestri. Nonlinear mirror mode-locking of a cw Nd:YLF laser. *Optics Letters*, 19:792–794, 1994.

[40] K. A. Stankov. A new mode-locking technique using a nonlinear mirror. *Optics Communications*, 66:41, 1988.

[41] K. A. Stankov. Pulse shortening by a nonlinear mirror mode locker. *Applied Optics*, 28:942–945, 1989.

[42] K. A. Stankov. Frequency domain analysis of the mode-locking process in a laser with a second-harmonic nonlinear mirror. *Optics Letters*, 16:639–641, 1991.

[43] A. Smith. Free software available at http://www.sandia.gov/imrl/X1118/xxtal.htm. 1999.

[44] K. A. Stankov. 25 ps pulses from a Nd:YAG laser mode locked by a frequency doubling BBO crystal. *Applied Physics Letters*, 58:2203–2204, 1991.

[45] V. Couderc, A. Barthelemy, V. Sakovich, and H. Jarlstrom. Anti-mode locked operation of a ps Nd:YAG laser using a second-order nonlinear mirror. In *International Symposium on Advanced Materials for Optics and Optoelectronics*, volume 2777. SPIE, Prague, 1995, pp. 210–216.

[46] A. Agnesi, C. Pennacchio, G. C. Reali, and V. Kubecek. High-power diode-pumped picosecond Nd^{3+}:YVO_4 laser. *Optics Letters*, 22:1645–1647, 1997.

[47] A. Agnesi, G. C. Reali, and V. Kubecek. Nonlinear mirror operation of a diode-pumped quasi-cw picosecond Nd:YAG laser. *Applied Physics B*, 66:283–285, 1998.

[48] A. Agnesi, G. C. Reali, and V. Kubecek. Nonlinear mirror operation of a diode-pumped quasi-cw picosecond Nd:YAG laser. Journal of the Optical Society of America B 16(8):1236–1239, 1999.

[49] V. Kubecek. Nonlinear mirror mode-locking of solid state lasers. volume 5259. SPIE, Bellingham, WA, 2003. pp. 403–410.

[50] [illegible] and G. McClain. Parametric mode locking. IEEE Journal of Quantum Electronics, QE-[illegible], 1992.

[51] K. A. Stankov. Negative feedback by using a nonlinear mirror for generation of long train of short pulses. Applied Physics B, 62:166–162, 1996.

[52] V. Kubecek, V. Couderc, B. Bourliaguet, F. Louradour, and A. Barthelemy. 4-W and 23-ps pulses from a lamp-pumped Nd:YAG laser passively mode-locked by polarization switching in a KTP crystal. Applied Physics B, 69:99–102, 1999.

[53] A. V. Babushkin, N. S. Vorob'ev, A. M. Prokhorov, and M. Y. Shchelev. Stable picosecond $YAlO_3$:Nd (YAP) laser with hybrid mode-locking and negative transient feedback utilizing a GaAs crystal. Soviet Journal of Quantum Electronics, 19:1310–1311, 1989.

[54] T. T. Dang, A. Stintz, J.-C. Diels, and Y. Zhang. Active solid state short pulse laser gyroscope. Volume available on CD from ION, 1800 Diagonal Road, Suite 480, Alexandria, VA 22314, Albuquerque, New Mexico, 2004. ION 60th Annual Meeting—Session D4.

[55] O. E. Martinez and L. A. Spinelli. Deterministic passive mode locking of solid-state lasers. Applied Physics Letters, 39:875–877, 1981.

[56] [illegible]. Highly stable subpicosecond [illegible] Nd^{3+} glass laser with passive mode-locking and negative feedback. Kvantovaya Elektronika, 15:[illegible]–1459, 1988.

[57] P. Heinz, W. Kriegleder, and A. Laubereau. Feedback control of an actively-passively mode-locked Nd:glass laser. Applied Physics A, 43:209–212, 1987.

[58] D. H. Auston, S. McAfee, C. V. Shank, E. P. Ippen, and O. Teschke. Picosecond spectroscopy of semiconductors. Solid State Electronics, 21:147, 1978.

[59] W. A. Schroeder, T. S. Stark, M. D. Dawson, T. F. Boggess, A. L. Smirl, and G. C. Valley. Picosecond separation and measurement of coexisting photo-refractive, bound-electronic, and free-carrier grating dynamics in GaAs. Optics Letters, 16:159–161, 1991.

[60] A. Agnesi, A. Guandalini, and G. Reali. Continuous passive mode-locked [illegible] low pump power Nd:YAG laser. In Europhysics Conference Abstracts, volume 28C, Lausanne, Switzerland, 2004.

[61] J. Schwartz, W. Weiler, and R. K. Chang. Laser-pulse shaping using inducible absorption with controlled q-switch time behavior. IEEE Journal of Quantum Electronics, QE-6:442–450, 1970.

[62] A. Hordvik. Pulse stretching utilizing two-photon-induced light absorption. IEEE Journal of Quantum Electronics, QE-6:199–203, 1970.

[63] A. Agnesi, A. Del Corno, J.-C. Diels, P. Di Trapani, M. Fogliani, V. Kubecek, G. C. Reali, C.-Y. Yeh, and X. M. Zhao. Generation of extended pulse trains of minimum duration by passive negative feedback applied to solid state Q-switched lasers. IEEE Journal of Quantum Electronics, 28:710–719, 1992.

[64] V. Kubecek, A. Dombrowski, J.-C. Diels, and A. Stintz. Mode-locked Nd:YAG laser with passive negative feedback using multiple quantum well saturable absorber. In Proceedings of SPIE, OC-NPL 2004, SPIE, Prague, Czech Republic, 2004, pp. 61–66.

[65] U. Keller, K. J. Weingarten, F. X. Kartner, D. Kopf, B. Braun, I. D. Jung, R. Fluck, C. Honninger, N. Matuschek, and J. Aus der Au. Semiconductor saturable absorber mirrors (SESAMs) for femtosecond to nanosecond pulse generation in solid-state lasers. IEEE Journal of Selected Topics in Quantum Electronics, 2:435–453, 1996.

[66] S. L. Chuang. Physics of Optoelectronic Devices. John Wiley & Sons, New York, 1995.

[67] P. W. Smith, Y. Silberberg, and D. A. B. Miller. Mode-locking of semiconductor diode lasers using saturable excitonic nonlinearities. *Journal of the Optical Society of America B* 2:1228–1235, 1985.

[68] P. J. Delfyett, L. Florez, N. Stoffel, T. Gmitter, N. Andreadakis, G. Alphonse, and W. Ceislik. 200 femtosecond optical pulse generation and intracavity pulse evolution in a hybrid mode-locked semiconductor diode laser/amplifier system. *Optics Letters* 17:670–672, 1992.

[69] S. Gupta, J. F. Whitaker and G. A. Mourou. Ultrafast carrier dynamics in III-V semiconductors grown by molecular-beam epitaxy at very low substrate temperatures. *IEEE Journal of Quantum Electronics* 28:2464–2472, 1992.

[70] R. C. Powell, S. A. Payne, L. L. Chase, and G. D. Wilke. Index-of-refraction change in optically pumped solid-state laser materials. *Optics Letters* 14:1204, 1989.

[71] M. Weitz, B. Stuart, R. Koeppe, R. Wallenstein, and D. Kreisch. In *CLEO*, *CThC*, Optical Society of America, DC, San Francisco, 2004.

[72] W. Koechner and M. Bass. *Solid-State Lasers*. Springer-Verlag, Berlin, Heidelberg, New York, 2003.

[73] B. Proctor and F. Wise. Time-resolved nonlinear reflection in femtosecond laser gain media. *Optics Letters* 23:1340–1342, 1998.

[74] P. F. Moulton. Spectroscopic and laser characteristics of $Ti:Al_2O_3$. *Journal of the Optical Society of America B* 3:125–133, 1986.

[75] D. E. Spence, P. N. Kean, and W. Sibbett. 60-fs pulse generation from a self-mode-locked Ti:sapphire laser. *Optics Letters* 16:42–44, 1991.

[76] M. T. Asaki, C. P. Huang, D. Garvey, J. Zhou, H. C. Kapteyn, and M. M. Murnane. Generation of 11-fs pulses from a self-mode-locked Ti:sapphire laser. *Optics Letters* 18:977–979, 1993.

[77] A. Stingl, Ch. Spielmann, F. Krausz, and R. Szipöcs. Generation of 11-fs pulses from a Ti:sapphire laser without the use of prisms. *Optics Letters* 19:204–206, 1994.

[78] J. Reichert, R. Holzwarth, T. Udem, and T. W. Hänsch. Measuring the frequency of light with mode-locked lasers. *Optics Communications* 172:59–68, 1999.

[79] H. R. Telle, G. Steinmeyer, A. E. Dunlop, J. Stenger, D. H. Sutter, and U. Keller. Carrier-envelope offset phase control: A novel concept for absolute optical frequency measurement and ultrashort pulse generation. *Applied Physics B* 69:327, 1999.

[80] S. A. Diddams, D. J. Jones, J. Ye, S. T. Cundiff, J. L. Hall, J. K. Ranka, R. S. Windeler, R. Holzwarth, T. Udem, and T. W. Hänsch. Direct link between microwave and optical frequencies with a 300 THz femtosecond laser comb. *Physical Review Letters* 84:5102–5105, 2000.

[81] U. Morgner, R. Ell, G. Metzler, T. R. Schibli, F. X. Kärtner, J. G. Fujimoto, H. A. Haus, and E. P. Ippen. Nonlinear optics with phase-controlled pulses in the sub-two-cycle regime. *Physical Review Letters* 86:5462–5465, 2001.

[82] F. X. Kärtner, N. Matuschek, T. Schibli, U. Keller, H. A. Haus, C. Heine, R. Morf, V. Scheuer, M. Tilsch, and T. Tschudi. Design and fabrication of double-chirped mirrors. *Optics Letters* 22:831–833, 1997.

[83] M. Ramaswamy, M. Ulman, J. Paye, and J. G. Fujimoto. Cavity-dumped femtosecond Kerr-lens mode-locked Ti:sapphire laser. *Optics Letters* 18:1822–1824, 1993.

[84] M. S. Pshenichnikov, W. P. de Boeij, and D. A. Wiersma. Generation of 13-fs, 5-MW pulses from a cavity-dumped Ti:sapphire laser. *Optics Letters* 19:572–574, 1994.

[85] J. Jasapara, V. L. Kalashnikov, D. O. Krimer, G. Poloyko, W. Rudolph, and M. Lenzner. Automodulations in Kerr-lens modelocked solid-state lasers. *Journal of the Optical Society of America B* 17:319–326, 2000.

[86] S. H. Cho, F. X. Kärtner, U. Morgner, E. P. Ippen, J. G. Fujimoto, J. E. Cunningham, and W. H. Knox. Generation of 90-nJ pulses with a 4-MHz repetition-rate Kerr-lens mode-locked Ti:sapphire oscillator. *Optics Letters* 26:560–562, 2001.

[87] A. Apolonski, A. Fernandez, T. Fuji, K. Krausz, A. Fürbach, and A. Stingl. Scalable high-energy femtosecond Ti:sapphire oscillator. In CLEO, CThM2, San Francisco, 2004. Optical Society of America.

[88] M. Stalder, M. Bass, and B. H. T. Chai. Thermal quenching of fluorescence in chromium-doped fluoride laser crystals. *Journal of the Optical Society of America B*, 9:2271–2273, 1992.

[89] V. Kamalov, R. Quintero-Torres, and J.-C. Diels. Ultralow-pump-threshold laser diode pumped Cr:LiSAF laser. In V. Ya. Panchenko, G. Huber, and A. Scherbakov, Eds., *Advanced Lasers and Systems*, volume 5137, SPIE, Bellingham, WA, 2003, pp. 43–47.

[90] G. J. Valentine, J. M. Hopkins, P. Loza-Alvarez, G. T. Kennedy, W. Sibbett, D. Burns, and A. Valster. Ultralow-pump-threshold, femtosecond Cr^{3+}:LiSrAlF$_6$. *Optics Letters*, 22:1639–1641, 1997.

[91] R. Szipöcs and A. Köházi-Kis. Theory and design of chirped dielectric laser mirrors. *Applied Physics B*, 65:115–135, 1997.

[92] I. T. Sorokina, E. Sorokin, E. Wintner, A. Cassanho, H. P. Jenssen, and R. Szipöcs. Sub-20 fs pulse generation from the mirror dispersion controlled LiSGaF and LiSAF lasers. *Applied Physics B*, 65:245–253, 1997.

[93] L. K. Smith, S. A. Payne, W. L. Kway, L. L. Chase, and B. H. T. Chai. Investigation of the laser properties of Cr^{3+}:LiSrGaF$_6$. *IEEE Journal of Quantum Electronics*, 28:2612–2618, 1992.

[94] D. Kopf, K. J. Weingarten, G. Zhang, M. Moser, M. A. Emanuel, R. J. Beach, J. A. Skidmore, and U. Keller. High-average-power diode-pumped femtosecond Cr:LiSAF lasers. *Applied Physics B*, 65:235–243, 1997.

[95] S. Uemura and K. Torizuka. Generation of 12-fs pulses from a diode-pumped Kerr-lens mode-locked Cr:LiSAF laser. *Optics Letters*, 24:780–782, 1999.

[96] I. T. Sorokina, E. Sorokin, E. Wintner, A. Cassanho, and H. P. Jenssen. 14-fs pulse generation in Kerr-lens mode-locked prismless LiSGaF and LiSAF lasers: Observation of pulse self-frequency shift. *Optics Letters*, 22:1716–1718, 1997.

[97] R. Mellish, R. Koch, and R. Wallenstein. Kerr lens mode-locked Cr:LiSAF laser pumped by the diffraction-limited output of a 672 nm diode laser master-oscillator power-amplifier system. *Journal of the Optical Society of America B*, 14:672–675, 1997.

[98] I. Thomann, A. Bartels, K. L. Corwin, N. R. Newbury, L. Hollberg, S. A. Diddams, J. W. Nicholson, and M. F. Yan. 420-MHz Cr:forsterite femtosecond ring laser and continuum generation in the 1–2 μm range. *Optics Letters*, 28:1368–1370, 2003.

[99] V. Petričević, S. K. Gayen, and R. R. Alfano. Laser action in chromium-activated forsterite for near-infrared excitation: is Cr^{4+} the lasing ion? *Applied Physics Letters*, 53:2590, 1988.

[100] A. Seas, V. Petričević, and R. R. Alfano. Self-mode-locked chromium-doped forsterite laser generates 50-fs pulses. *Optics Letters*, 18:891–893, 1993.

[101] V. Petričević, A. B. Bykov, J. M. Evans, and R. R. Alfano. Room-temperature near-IR tunable lasing operation of Cr^{4+}:Ca$_2$GeO$_4$. *Optics Letters*, 21:1750–1752, 1996.

[102] A. Xu, J. M. Evans, V. Petričević, S. P. Guo, O. Maksimov, M. C. Tamargo, and R. R. Alfano. Continuous-wave and passively mode-locked operation of a cunyite laser. Applied Optics, [illegible], 2001.

[103] L. Qian, X. Liu, and F. Wise. Cr:forsterite laser pumped by broad-area laser diodes. *Optics Letters*, 22:1707–1709, 1997.

[104] C. Chudoba, J. G. Fujimoto, E. P. Ippen, H. A. Haus, U. Morgner, F. X. Kärtner, V. Scheuer, G. Angelow, and T. Tschudi. All-solid-state Cr:forsterite laser generating 14 fs pulses at 1.3 μm. *Optics Letters*, 26:292–294, 2001.

[105] V. Yanovsky, Y. Pang, F. Wise, and B. I. Minkov. Generation of 25-fs pulses from a self-mode-locked Cr:forsterite laser with optimized group-delay dispersion. *Optics Letters*, 18:1541–1543, 1993.

[106] I. Thomann, L. Hollberg, S. A. Diddams, and R. Equall. Chromium-doped forsterite: Dispersion measurement with white-light interferometry. *Applied Optics*, 42:1661, 2003.

[107] J. M. Evans, V. Petricevic, A. B. Bykov, and R. R. Alfano. Direct diode-pumped continuous-wave near-infrared tunable laser operation of Cr^{4+}:forsterite and $Cr^{4+}:Ca_2GeO_4$. *Optics Letters*, 22:1171–1173, 1997.

[108] R. Adair, L. L. Chase, and S. A. Payne. Nonlinear refractive index of optical crystals. *Physical Review B*, 39:3337–3350, 1989.

[109] W. F. Krupke, M. D. Shinn, J. E. Marion, J. A. Caird, and S. E. Stokowski. Spectroscopic, optical, and thermomechanical properties of neodymium- and chromium-doped gadolinium scandium gallium garnet. *Journal of the Optical Society of America B*, 3:102, 1986.

[110] T. Kushida, H. M. Marcos, and J. E. Geusic. Laser transition cross section and fluorescence branching ratio for Nd^{3+} in yttrium aluminum garnet. *Physical Review*, 167:289, 1968.

[111] A. Umbrasas, J. C. Diels, G. Valiulis, J. Jacob, and A. Piskarskas. Generation of femtosecond pulses through second harmonic compression of the output of a Nd:YAG laser. *Optics Letters*, 20:2228–2230, 1995.

[112] A. Umbrasas, J. C. Diels, J. Jacob, and A. Piskarskas. Parametric oscillation and compression in KTP crystals. *Optics Letters*, 19:1753–1755, 1994.

[113] J. Biegert, V. Kubecek, and J. C. Diels. A new femtosecond UV source based on Nd:YAG. In *CLEO, 1999*, Optical Society of America, Baltimore, MD, 1999. p. 470.

[114] A. Giesen, H. Hügel, A. Voss, K. Wittig, U. Brauch, and H. Opower. Scalable concept for diode-pumped high-power solid-state lasers. *Applied Physics B*, 58:365, 1994.

[115] G. J. Spühler, T. Südmeyer, R. Paschotta, M. Moser, K. J. Weingarten, and U. Keller. Passively mode-locked high-power Nd:YAG lasers with multiple laser heads. *Applied Physics B*, 71:19–25, 2000.

[116] E. Innerhofer, T. Südmeyer, F. Brunner, R. Häring, A. Aschwanden, and R. Paschotta. 60 W average power in 810 fs pulses from a thin disk Yb:YAG laser. *Optics Letters*, 28:367–369, 2003.

[117] A. Agnesi and G. C. Reali. Development of medium power, compact ultrashort-pulse lasers. *Rivista del Nuovo Cimento*, 20(4):1–71, 1997.

[118] J. R. Lincoln and A. I. Ferguson. All-solid-state self-mode-locking of a Nd:YLF laser. *Optics Letters*, 19:2119–2121, 1994.

[119] R. Fluck, G. Zhang, U. Keller, K. J. Weingarten, and M. Moser. Diode-pumped passively mode-locked 1.3 μm $Nd:YVO_4$ and Nd:YLF lasers by use of semiconductor saturable absorbers. *Optics Letters*, 21:1378–1380, 1996.

[120] L. Turi and T. Juhasz. High-power longitudinally end-diode-pumped Nd:YLF regenerative amplifier. *Optics Letters*, 20:154–156, 1995.

[121] R. L. Fork and C. V. Shank. Generation of optical pulses shorter than 0.1 ps by colliding pulse mode-locking. *Applied Physics Letters*, 38:671, 1981.

[122] A. Finch, G. Chen, W. Sleat, and W. Sibbett. Pulse asymmetry in the colliding-pulse mode-locked dye laser. *Journal of Modern Optics*, 35:345–349, 1988.

[123] H. Kubota, K. Kurokawa, and M. Nakazawa. 29 fs pulse generation from a linear cavity synchronously pumped dye laser. *Optics Letters*, 13:749–751, 1988.

[124] J. C. Diels. Femtosecond dye lasers. In F. Duarte and L. Hillman, Eds., *Dye Laser Principles: With Applications*, Academic Press, Boston, MA, 1990. pp. 41–132.

[125] A. E. Siegman. An antiresonant ring interferometer for coupled laser cavities, laser output coupling, mode-locking, and cavity dumping. *IEEE Journal of Quantum Electronics*, QE-9:247–250, 1973.

[126] M. C. Nuss, R. Leonhardt, and W. Zinth. Stable operation of a synchronously pumped colliding-pulse mode-locking dye laser. *Optics Letters*, 10:16–18, 1985.

[127] F. J. Duarte and R. O. James. Tunable solid-state lasers incorporating dye-doped, polymer-nanoparticle gain media. *Optics Letters*, 28:2088–2090, 2003.

[128] F. J. Duarte and R. O. James. Spatial structure of dye-doped polymer nanoparticle laser media. *Applied Optics*, 43:4088–4090, 2004.

[129] Z. Bor and A. Müller. Picosecond distributed feedback dye lasers. *IEEE Journal of Quantum Electronics*, QE-22:1524–1533, 1986.

[130] S. Szatmári and F. P. Schäfer. Generation of high power UV femtosecond pulses. In T. Yajima, K. Yoshihara, C. B. Harris, and S. Shionoya, Eds., *Ultrafast Phenomena VI*, Springer-Verlag, Berlin, Germany, 1988, p. 63–66.

[131] P. H. Chiu, P. Pax, L. Marshall, F. Wilson, and R. Aubert. A high-energy, electromagnetically tuned single mode, short-cavity picosecond dye laser system: Design and performance. *Optics and Lasers in Engineering*, 10:23–44, 1989.

[132] H. P. Kuo, A. J. Cox, G. W. Ross, D. W. Gallaux, H. Hamel, R. W. Yeh, S. P. Tonge, and J. H. Clark. Amplification of tunable, picosecond pulses from a single mode, short cavity dye laser. *IEEE Journal of Quantum Electronics*, QE-21:1797–1805, 1985.

[133] P. Simon, S. Szatmári, and F. P. Schäfer. Generation of 30 fs pulses tunable over the visible spectrum. *Optics Letters*, 16:1569–1571, 1991.

[134] P. P. Vasil'ev. Ultrashort pulse generation in diode lasers. *Optical and Quantum Electronics*, 24:801–824, 1992.

[135] G. A. Alphonse, D. B. Gilbert, M. G. Harvey, and M. Ettenberg. High-power superluminescent diodes. *IEEE Journal of Quantum Electronics*, 24:2454–2457, 1988.

[136] P. J. Delfyett, Y. Silberberg, G. A. Alphonse, and W. Ceislik. Hot-carrier thermalization induced self-phase modulation in semiconductor traveling wave amplifiers. *Applied Physics Letters*, 59:10, 1991.

[137] P. J. Delfyett, C. H. Lee, L. Florez, N. Stoffel, T. Gmitter, N. Andreadakis, G. Alphonse, and J. C. Connolly. Generation of subpicosecond high-power optical pulses from a hybrid mode-locked semiconductor laser. *Optics Letters*, 15:1371–1373, 1990.

[138] S. Chen and J. Wang. Self-starting issues of passive self-focusing mode locking. *Optics Letters*, 16:1689–1691, 1991.

[139] C. F. Lin and C. L. Tang. Colliding pulse mode-locking of a semiconductor laser in an external ring cavity. *Applied Physics Letters*, 62:1053–1055, 1993.

[140] W. Rudolph and B. Wilhelmi. *Light Pulse Compression*. Harwood Academic, Chur, London, 1989.

[141] B. Zysset, P. Beaud, and W. Hodel. Generation of optical solitons in the wavelength region 1.37–1.49 µm. *Applied Physics Letters*, 50:1027–1029, 1987.

[142] J. D. Kafka and T. Baer. Fiber Raman soliton laser pumped by a Nd:YAG laser. *Optics Letters*, 12:181–183, 1987.

[143] A. S. Gouveia-Neto, A. S. L. Gomes, and J. R. Taylor. Generation of 33 fs pulses at 1.32 µm through a high order soliton effect in a single mode optical fiber. *Optics Letters*, 12:395–397, 1987.

[144] I. N. Duling III. Subpicosecond all-fibre erbium laser. *Electronics Letters*, 27:544–545, 1991.

[145] I. N. Duling. All-fiber ring soliton laser mode locked with a nonlinear mirror. *Optics Letters*, 16:539–541, 1991.

[146] R. P. Craig-Ryan and B. J. Ainslie. Glass structure and fabrication techniques. In P. W. France, Ed., *Optical Fibre Lasers and Amplifiers*, Blackie & Son, Ltd., Glasgow, Scotland, 1991, pp. 50–78.

[147] I. N. Duling, R. P. Moeller, W. K. Burns, C. A. Villarruel, L. Goldberg, E. Snitzer, and H. Po. Output characteristics of diode pumped fiber ASE sources. *IEEE Journal of Quantum Electronics*, 27:995–1003, 1991.

[148] M. Hofer, M. E. Fermann, F. Haberl, M. H. Ober, and A. J. Schmidt. Mode locking with cross-phase and self-phase modulation. *Optics Letters*, 16:502–504, 1991.

[149] K. J. Blow and D. Wood. Theoretical description of transient stimulated Raman scattering in optical fibers. *IEEE Journal of Quantum Electronics*, 25:2665–2673, 1989.

[150] M. Hofer, M. E. Fermann, F. Haberl, M. H. Ober, and A. J. Schmidt. Characterization of ultrashort pulse formation in passively mode-locked fiber lasers. *Optics Letters*, 16:502–504, 1991.

[151] K. J. Blow and D. Wood. Theoretical description of transient stimulated Raman scattering in optical fibers. *IEEE Journal of Quantum Electronics*, 25:2665–2673, 1989.

[152] M. Hofer, M. E. Fermann, F. Haberl, M. H. Ober, and A. J. Schmidt. Characterization of ultrashort pulse formation in passively mode-locked fiber lasers. *Optics Letters*, 16:502–504, 1991.

[153] K. J. Blow and D. Wood. Theoretical description of transient stimulated Raman scattering in optical fibers. *IEEE Journal of Quantum Electronics*, 25:2665–2673, 1989.

[154] M. Hofer, M. E. Fermann, F. Haberl, M. H. Ober, and A. J. Schmidt. Characterization of ultrashort pulse formation in passively mode-locked fiber lasers. *Optics Letters*, 16:502–504, 1991.

[155] K. J. Blow and D. Wood. Theoretical description of transient stimulated Raman scattering in optical fibers. *IEEE Journal of Quantum Electronics*, 25:2665–2673, 1989.

[156] M. Hofer, M. E. Fermann, F. Haberl, M. H. Ober, and A. J. Schmidt. Characterization of ultrashort pulse formation in passively mode-locked fiber lasers. *Optics Letters*, 16:502–504, 1991.

[157] K. J. Blow and D. Wood. Theoretical description of transient stimulated Raman scattering in optical fibers. *IEEE Journal of Quantum Electronics*, 25:2665–2673, 1989.

[158] M. Hofer, M. E. Fermann, F. Haberl, M. H. Ober, and A. J. Schmidt. Characterization of ultrashort pulse formation in passively mode-locked fiber lasers. *Optics Letters*, 16:502–504, 1991.

[159] K. J. Blow and D. Wood. Theoretical description of transient stimulated Raman scattering in optical fibers. *IEEE Journal of Quantum Electronics*, 25:2665–2673, 1989.

[160] M. Hofer, M. E. Fermann, F. Haberl, M. H. Ober, and A. J. Schmidt. Characterization of ultrashort pulse formation in passively mode-locked fiber lasers. *Optics Letters*, 16:502–504, 1991.

[161] K. J. Blow and D. Wood. Theoretical description of transient stimulated Raman scattering in optical fibers. *IEEE Journal of Quantum Electronics*, 25:2665–2673, 1989.

[162] M. Hofer, M. E. Fermann, F. Haberl, M. H. Ober, and A. J. Schmidt. Characterization of ultrashort pulse formation in passively mode-locked fiber lasers. *Optics Letters*, 16:502–504, 1991.

[163] K. J. Blow and D. Wood. Theoretical description of transient stimulated Raman scattering in optical fibers. *IEEE Journal of Quantum Electronics*, 25:2665–2673, 1989.

[164] M. Hofer, M. E. Fermann, F. Haberl, M. H. Ober, and A. J. Schmidt. Characterization of ultrashort pulse formation in passively mode-locked fiber lasers. *Optics Letters*, 16:502–504, 1991.

[165] K. J. Blow and D. Wood. Theoretical description of transient stimulated Raman scattering in optical fibers. *IEEE Journal of Quantum Electronics*, 25:2665–2673, 1989.